1. Report No.	2. Government Accession No.	3. Recipient's Catalog No.
NASA CR-159405		

4. Title and Subtitle	5. Report Date
Filling of Orbital Fluid Management Systems	August 1978
	6. Performing Organization Code

7. Author(s)	8. Performing Organization Report No.
E. C. Cady and H. H. Miyashiro	MDC G7374
	10. Work Unit No.

9. Performing Organization Name and Address	11. Contract or Grant No.
McDonnell Douglas Astronautics Company 5301 Bolsa Avenue Huntington Beach, California 92647	NAS 3-21022
	13. Type of Report and Period Covered
12. Sponsoring Agency Name and Address	Final Report-August 1977 to March 1978
NASA Lewis Research Center, Cleveland, Ohio	14. Sponsoring Agency Code

15. Supplementary Notes

Project Manager, John C. Aydelott, NASA Lewis Research Center, Cleveland, Ohio

16. Abstract

A comprehensive program was conducted to study, analytically, the gravity-dependent refill phenomena for a small-scale tank containing a screen acquisition device suitable for a Spacelab cryogenic fluid management experiment. The analysis is suitable for screen channel and screen liner devices and storable and cryogenic propellants. The analysis considers chill-down, interface stability, screen device and tank filling processes, ullage pressure control, and venting. The processes involved in low-g filling were examined and modelling techniques, appropriate to the experimental evaluation of critical filling phenomena, were defined as well as the overall ground and low-g experimental program.

17. Key Words (Suggested by Author(s))	18. Distribution Statement
Orbital fluid transfer Screen acquisition systems Cryogenic fluids Refill analysis	Unclassified-Unlimited

19. Security Classif. (of this report)	20. Security Classif. (of this page)	21. No. of Pages	22. Price*
Unclassified	Unclassified		

* For sale by the National Technical Information Service, Springfield, Virginia 22161

PREFACE

This report was prepared by McDonnell Douglas Astronautics Company under Contract NAS3-21022. The contract is administered by the National Aeronautics and Space Administration, Lewis Research Center, Cleveland, Ohio. The NASA Project Manager for the contract is Mr. John C. Aydelott. This final report describes technical efforts on the contract performed from August 1977 through March 1978.

CONTENTS

SYMBOLS

A, B	Experimentally determined constants
a	Screen surface area to unit volume ratio (1/m), acceleration (g's)
A	Area (m^2)
C_p	Specific heat at constant pressure (joule/gm-K)
D, d	Diameter (m)
f	Friction factor, $\frac{H_f^2 \, g_c}{\frac{L}{D_h} V^2}$, chilldown efficiency factor
g	Acceleration level (g's)
g_c	Gravitational constant (9.806 m/sec^2)
h	Heat transfer coefficient (joule/m^2-sec-K), head (m)
h_{fg}	Heat of vaporization (joule/kg)
k	Thermal conductivity (joule/m-sec-K)
L	Length (m)
M	Mass (kg)
N	Number of pleats
Nu	Nusselt number, $\frac{hD}{k}$
P	Pressure (N/m^2)
Pr	Prandl number, $\frac{C_p \mu}{k}$
ΔP	Pressure loss (N/m^2)
$\dot{q}$	Heat flux (watt/m^2)
$\dot{Q}$	Volumetric flow rate (m^3/sec), heating rate (watt)

R	Radius (m), gas constant
Re	Reynolds number, $\frac{\rho V D_h}{\mu}$, $\frac{\rho V}{\mu a^2 D}$
S	Annulus spacing, channel height (m)
t	Time (sec)
T	Temperature (K)
V	Fluid velocity (m/sec)
VOL	Volume (m^3)
$\dot{W}$	Weight flow rate (kg/sec)
W	Weight (kg)
We	Weber number, $\frac{\rho V^2 L}{\sigma}$
α	Wicking angle
Δ	Differential
ϵ	Screen void fraction
η	Efficiency
μ	Viscosity (N-sec/m^2)
ρ	Density (kg/m^3)
σ	Surface tension (dyne/cm), specific chilldown liquid requirement
θ	Angle (rad)

Subscripts

BAF, B	Baffle
C	Channel
chill	Chilldown
D	Dynamic
equip	Equipment
f	Frictional, fluid
h	Hydraulic, head
HE	Heat exchanger

i	Inside
in	Inlet
j	jth segment
min	minimum
P	Pleated
out	Outlet
o	Outside
S	Static, screen
ST	Capillary
T	Tank, total
U	Ullage
w	Tube wall, wicking
1	Screen inlet

INTRODUCTION

The application of screen devices to exploit surface tension forces and provide fluid control in low gravity has been demonstrated with storable propellants on satellites. These devices are also being developed for use with storables in the orbital maneuvering and attitude control systems of the Space Transportation System (STS) Orbiter Vehicle. For cryogenic fluids, such as liquid hydrogen (LH_2), the integration of the necessary thermal protection and vent systems with the screen device has not been developed sufficiently to confidently allow their use. Instead, for smaller-scale cryogen systems, storing the cryogen at supercritical pressures is common practice to provide historically proven (e.g., Apollo) single-phase fluid expulsion in low gravity. Storage of cryogens at supercritical pressures has, as its principal drawbacks, the requirements for heavy high-pressure storage vessels and substantial (electrical) power input to maintain constant tank pressure during supercritical fluid withdrawal. Many applications for cryogenic fluids in space require saturated or subcooled cryogenic liquids. To satisfy this need, NASA-Lewis Research Center (LeRC) has a reduced-gravity fluid management technology program. One of its objective is to provide the technology for efficient storage, acquisition, supply, and transfer of saturated or subcooled cryogenic liquids in space.

As a result of the program much of the technology associated with the storage, acquisition, and supply aspects of orbital cryogenic fluid management systems is in hand (References 1-6). The program culminated with a proposed Spacelab Cryogenic Fluid Management Experiment (SCFME) (Reference 7) to demonstrate orbital storage, acquisition, and supply of LH_2, but, to date, the receiver aspects of cryogenic fluid transfer have not been adequately addressed.

The program described herein studies the gravity-dependent refill phenomena for a small-scale (~ 1.0 m dia) LH_2 tank containing a screen acquisition device and suitable for a SCFME. The filling analysis is specifically oriented

toward the channel-type and full-pleated-liner-type screen devices defined for the SCFME in Reference 7, but is also suitable for propellant fluids other than LH_2 such as MMH, N_2O_4, and LO_2. The analysis relates fluid properties and screen acquisition systems' characteristics to the acceleration environment and predicts fluid fill quantity and requirements. It also considers simultaneous chilldown and filling, precooling followed by filling, and refilling of a fluid management system containing a liquid filled screen device.

In addition to the analysis, methods were examined for modelling critical aspects of the tank filling phenomena to define appropriate techniques for experimental verification of the analysis. Also defined was the total program needed to evaluate experimentally all critical aspects of orbital fluid management system filling, including ground and orbital testing. The experiment program definition includes conceptual design of the apparatus, approximate costs, and appropriate test program operations.

ANALYSIS OF FLUID MANAGEMENT SYSTEM FILLING

The objective of this task was to analyze the filling of a fluid management system by relating the fluid properties, liquid inflow rates, storage tank temperature and pressure, and the screen liquid acquisition system characteristics in a low and zero-g environment in order to predict the quantity of fluid required for filling and the maximum obtainable fill level of the fluid storage system.

The two-screen liquid acquisition devices, conceptually designed in Reference 7 and illustrated in Figure 1, are modelled.

CR19

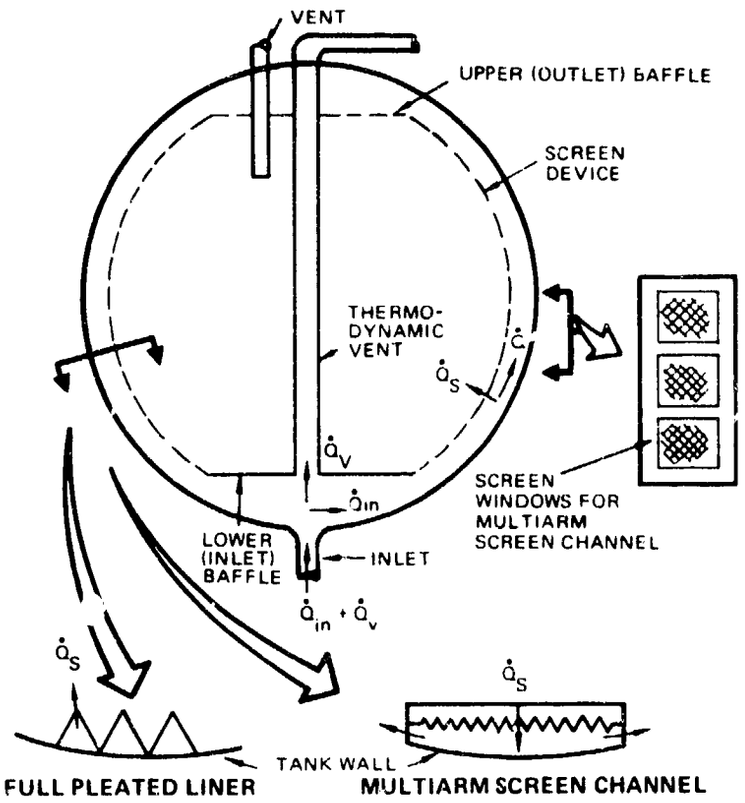

Figure 1. Screen Liquid Acquisition Devices Schematic

The analysis distinguishes between cryogenic and storable propellants only for those aspects unique to a cryogenic fluid such as the chilldown analysis and the thermodynamic vent system. Although the analysis was specifically tailored for the cryogenic propellants LH_2 and LO_2 and the storable propellants MMH and N_2O_4, it is applicable for any fluid because all fluid properties are inputs.

Because the analysis does not include the effects of the supply system and transfer line, the fluid at the inlet to the system is assumed to be liquid. Furthermore, the flowrate into the system is assumed to be constant with a varying supply pressure to provide a system in pressure and flow equilibrium.

The analysis is programmed in the Fortran IV language on the McDonnell Douglas Automation Company (MCAUTO) CDC CYBER 74 computer system. The math model options are tabulated in Table 1. The major assumptions and limitations of the math model are summarized in Table 2.

The math model is identified by MDAC Computer Program number P5762. Figure 2 is a logic flow diagram showing the calling sequence of the subroutines, the critical decision points, and the basic function of the subroutines. The logic, identified by the name CONTROL, calls the subroutines, makes decisions, initializes a number of variables, and performs a few calculations.

The math model logic consists of four basic parts (see Figure 2):

1. System chilldown
2. Screen device filling
3. Tank fill - forming of ullage bubble
4. Tank fill - ullage bubble formed

This breakdown was possible because of the assumptions made in the analysis, for example, the system is completely chilled down before liquid collects in the acquisition device and the acquisition device is filled before flow through the screen surfaces starts. These assumptions are later justified in the discussion of the subroutines. The following is a brief summary of the events and calculations that occur during the filling of the fluid management system.

The system chilldown analysis computes the required chilldown mass and chilldown time.

Table 1

SUMMARY OF MATH MODEL OPTIONS

Type of Fill:	1. Simultaneous chilldown and fill 2. Precooled tank fill 3. Fill with liquid in screen device
Type of Screen:	1. Full-pleated liner 2. Multiarm screen channel
Type of Ullage:	1. Constant pressure and temperature 2. Compression with no heat or mass transfer 3. Thermodynamic vent
Ullage Configuration:	1. One-component (vapor) 2. Two-component (vapor and pressurizing gas)
Type of Input and Output Data Units:	1. Metric input and output 2. English input and output 3. Metric input and English output 4. English input and metric output

The screen device filling analysis verifies the stability of the liquid-vapor interface in the screen device, determines the inlet static pressure required to provide a constant flowrate and system pressure balance, calculates the ullage conditions, and determines the time to fill or wickover the screen device and the trapped gas volume in the screen device.

The logic describing the formation of the ullage bubble during tank fill: (1) verifies the stability of the liquid-vapor interface for flow through the screen into the tank, (2) determines the inlet static pressure required to provide a constant flowrate, (3) calculates the flow and pressure distribution in the screen device and through the screen, (4) calculates the ullage condition, and (5) determines the appropriate time to form the ullage bubble.

Table 2

SUMMARY OF MATH MODEL ASSUMPTIONS/LIMITATIONS

Assumptions/Limitations	Comments
1. Constant liquid and gas properties	Changes in liquid and gas properties cannot be accounted for because of changes in the ullage and inlet pressures. Should not adversely affect the results of the analysis except for large changes in pressure and/or temperature, therefore, care should be exercised in interpreting the results for large changes in pressures and/or temperatures.
2. Low g acceleration direction is towards the inlet	Orientation of the fluid management system is restricted by the gravitational environment.
3. Two types of screen devices A. Full pleated liner B. Multiarm screen channel	Analysis of other screen device configuration would require math model modifications.
4. Stable liquid vapor interface exists throughout	The calculations will be terminated if the stability criteria are violated. May require low inflow rates depending on system size, fluid properties, and stability criteria.
5. Inflow rate is an input constant	The inlet static pressure is computed to provide a system in pressure and flow equilibrium.
6. System is chilled down before liquid enters the system.	The configuration of the system must be capable of satisfying this assumption.
7. Screen device is filled before liquid starts to flow into the tank	System size and acceleration levels are limited to assure screen device fill before screen flow through.
8. Ullage bubble is formed when the pleats or channel gap is filled	Only a time approximation that may be useful in interpreting the analytical results.
9. Ullage bubble is spherical or near spherical	Bond number is the order of unity.
10. Compression with no heat and mass transfer	Care must be exercised in interpreting the results of the analysis if the system temperature changes are large.
11. Thermodynamic vent fluid is in the annular flow regime	If the flow is in another flow regime (i.e., mist flow) the heat exchange can be accounted for by the efficiency factor included in the analysis or the analysis can be revised.
12. Thermodynamic vent effective length is the portion exposed to the ullage	No heat exchange between the liquid and thermodynamic vent, therefore, subcooling of the liquid is not accounted for and the heat transfer between the ullage and thermodynamic vent may be optimistic.
13. Pseudo-steady state analysis in time	The changes in system parameters (i.e., pressure and temperature) should not be large over each time increment.
14. Maximum of two components in the ullage	The two components should consist of the liquid vapors and a pressurizing gas.

CR19

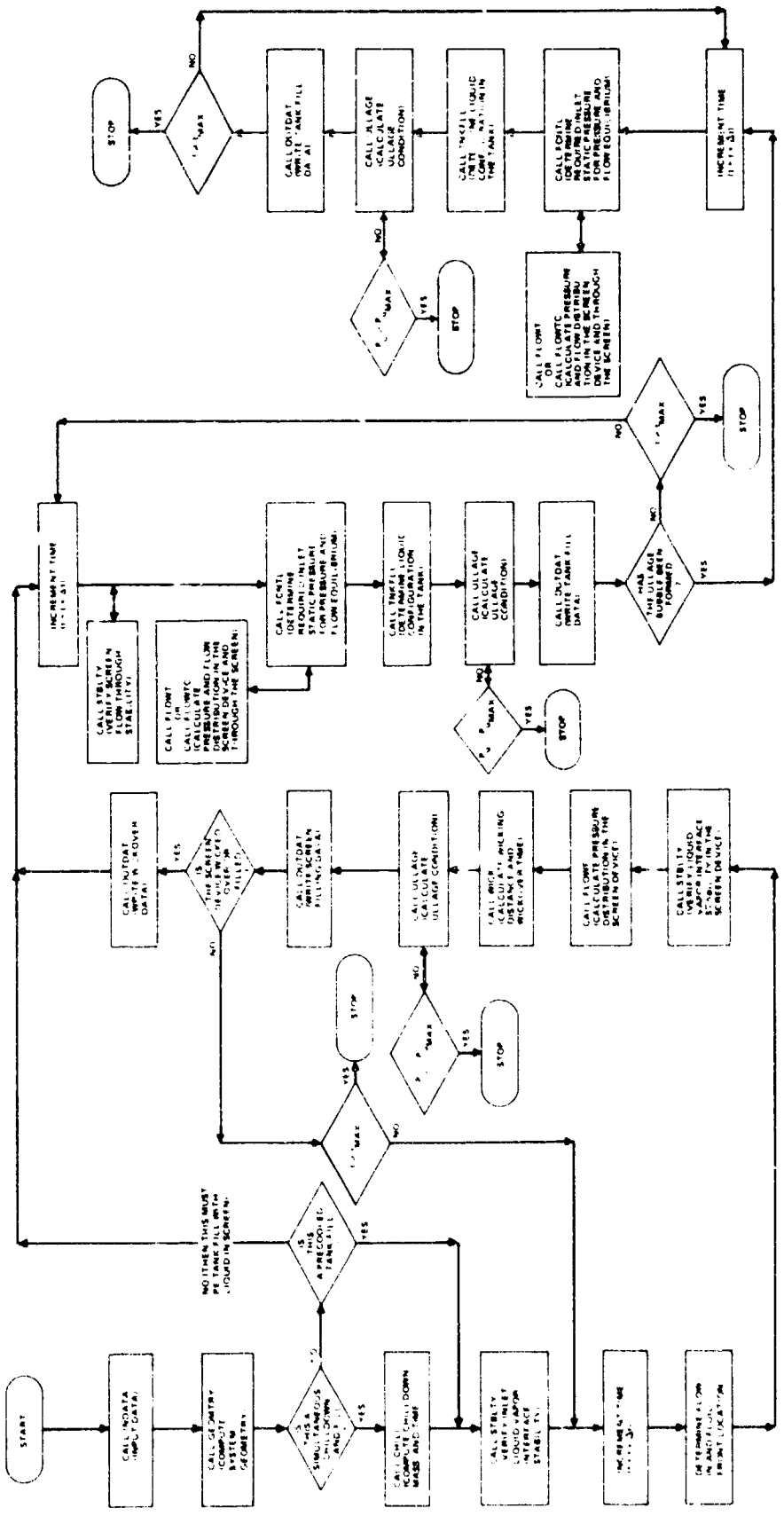

Figure 2. P5762 Logic Flow Diagram

The logic describing the tank fill after the ullage bubble is formed: (1) determines the inlet static pressure required to provide a constant flowrate, (2) calculates the flow and pressure distribution in the screen device and through the screen, and (3) calculates the ullage condition and bubble diameter.

The following sections describe the various subroutines used in the analysis and indicate the pertinent equations used. The inputs to the math model consist of the fluid properties, system geometry, initial system pressure, and temperature and math model options.

SUBROUTINE CHILL

Subroutine CHILL calculates the mass of liquid required to chilldown the tank, screen device, baffle, and other plumbing expressed by (see symbols):

$$M_{chill} = f \, \phi_{min} \, M_{equip} \tag{1}$$

and the chilldown time expressed by

$$t_{chill} = M_{chill} / \dot{Q}_{chill} \tag{2}$$

The chilldown mass model was developed in Reference 8. The factor f is included to account for chilldown inefficiencies that might occur and will be useful to correlate test data. The specific liquid requirements, ϕ, for LH_2 and LO_2 required to chilldown aluminum are shown in Figures 3 and 4, respectively. The minimum specific liquid requirement, ϕ_{min} corresponds to the liquid required to cool the system to its operating condition if all of the refrigeration available in the liquid is used. The maximum specific liquid requirement, ϕ_{max} corresponds to the liquid required to cool the system to its operating condition if only the refrigeration available in the latent heat of vaporization of the liquid is used.

In the configuration of the Spacelab fluid management system all of the metallic mass to be chilled down inside the tank is concentrated in the tank wall and screen device and all of the initial fluid inflow is confined to the screen

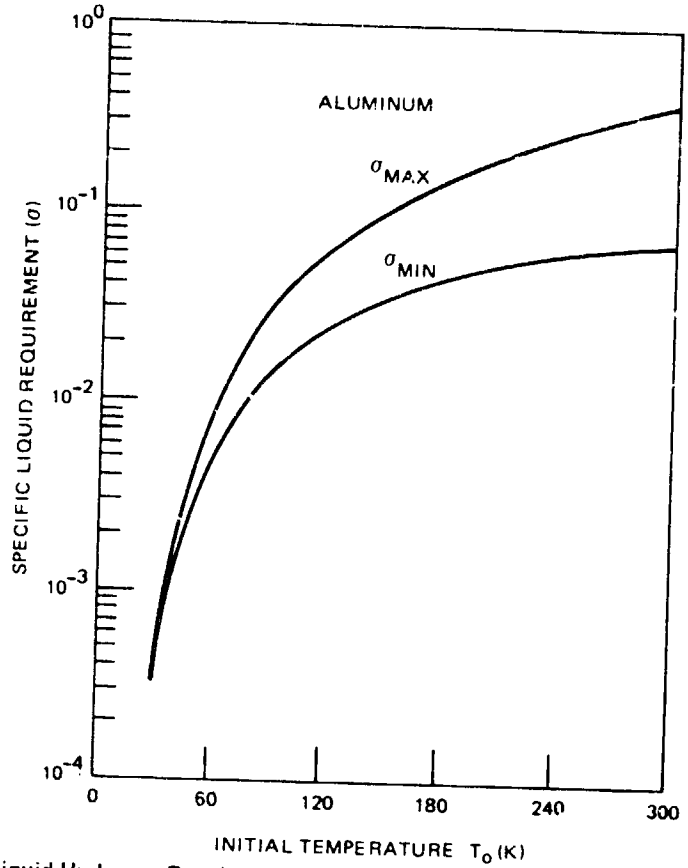

Figure 3. Specific Liquid-Hydrogen Requirement for Cool-Down as a Function of Initial Equipment Temperature

annulus or channel. With the liner, all of the vaporized fluid (gas) will flow naturally along the annulus (in contact with wall and liner) and through the liner, using all its heat capacity for chilldown. Similarly, for the channel configuration, the vaporized inflow will flow through the screen and along the tank wall. also using all of its heat capacity. Because of the configurations and the low inflow rates, it is assumed that the chilldown process closely approximates the case where the minimum chilldown fluid requirements occur because the chilldown fluid exits the system at equipment temperature.

It is assumed that liquid filling does not take place until the fluid management system is effectively chilled down because of the low inflow rates and the efficient thermal and flow barrier presented by the screen device.

The assumption is further justified; the energy that must be absorbed by the chilldown fluid for aluminum rapidly drops with decreasing temperature,

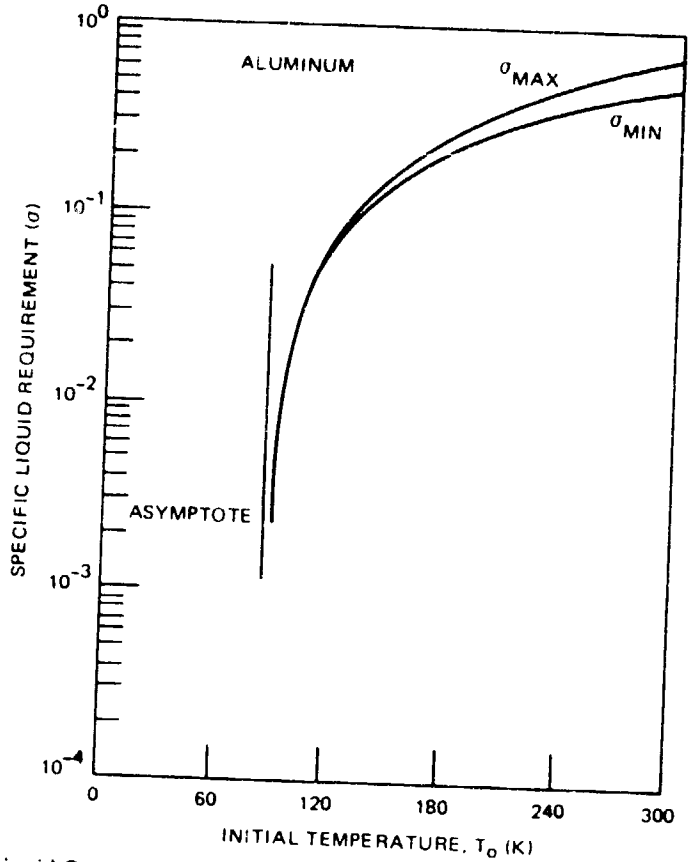

Figure 4. Specific Liquid-Oxygen Requirement for Cool-Down as a Function of Initial Equipment Temperature

as shown in Figure 5. Note that at 100 K (180°) only 10% of the room temperature energy remains, and at 50 K (90°R) only 1%. At this metal temperature, LH_2 will still be film-boiling vigorously, but almost no energy will be left in the system. To reduce the temperature of aluminum from 32 K (57°R) to 26 K (47°R) [saturated liquid hydrogen temperature at 413700 n/m^2 (60 psia)], requires the removal of only 0.14% of the aluminum's room temperature energy. For the other cryogenic fluid considered in this analysis, liquid oxygen, the last 6K of temperature decrease requires the removal of 1.5% of the aluminum's room temperature energy, hence, very litt energy is left in the system for either cryogenic fluid.

SUBROUTINE FCNTL

The screen flow-through models, subroutines FLØWT and FLØWTC, require pressure and flow distribution convergence. The pressure at the screen flow-through front must be balanced with the downstream pressure and the

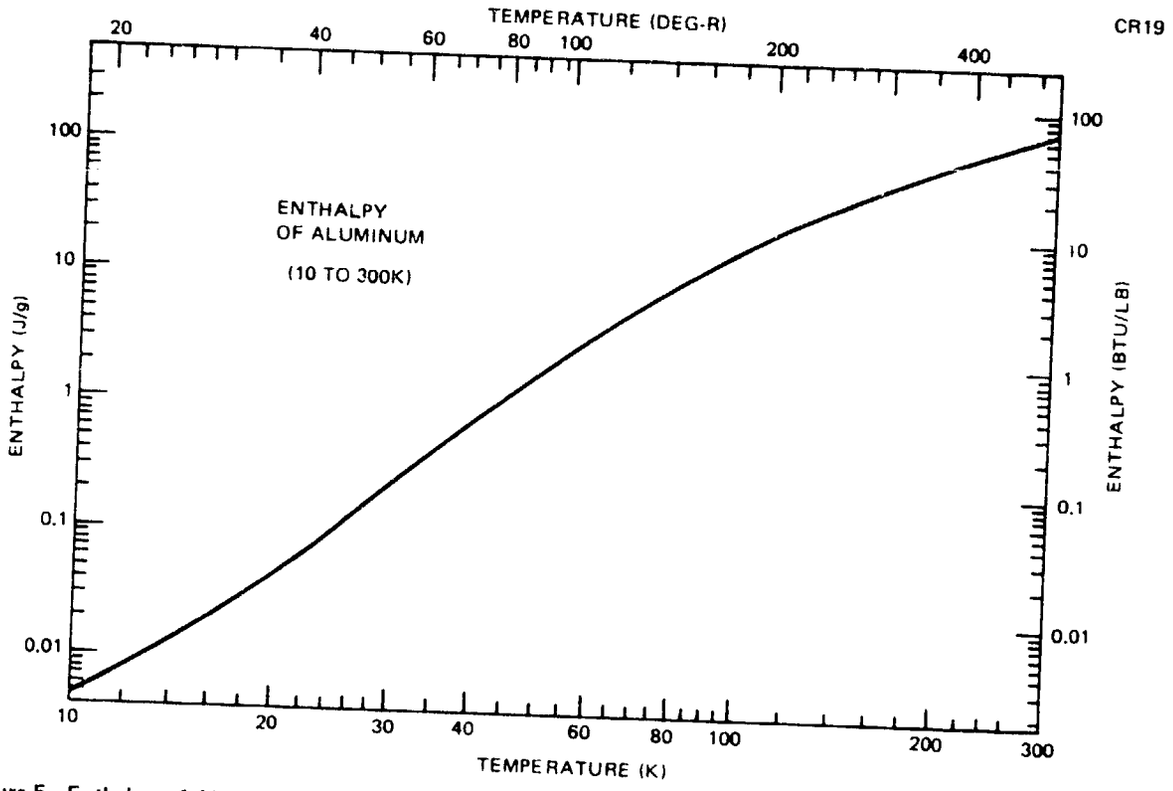

Figure 5. Enthalpy of Aluminum Versus Temperature

total flowrate through the screen device must equal the inflow rate. Because the analysis is pseudo-steady-state over time and the pressures in each screen segment are constant (at the inlet value), absolute pressure convergence cannot be achieved except by coincidence, so subroutine FCNTL was developed to minimize the error in the pressure convergence scheme. Pressure convergence occurs if one of the following criteria is satisfied:

1. The pressure difference across the screen at the flow-through front is within a specified limit (input as CØNVGP).
2. The change in the flow-through-front angle as the inlet static pressure changes is within a specified limit (input as CØNVGA).
3. There is no change in the flow-through-front location as the inlet static pressure changes.

SUBROUTINE FLØWF

Subroutine FLØWF determines the pressure distribution in the screen device (full pleated liner and multiarm screen channel) during screen device filling.

The basic assumption made is that the pressure across the fluid front must be balanced. In other words, at the fluid front, the ullage pressure is equal to the fluid static pressure plus the capillary pressure (See Figure 6). That is:

$$P_U = P_S + P_{ST} \tag{3}$$

The capillary pressure is defined as:

$$P_{ST} = \sigma\left(\frac{1}{R_1} + \frac{1}{R_2}\right) \tag{4}$$

where R_1 and R_2 are the principal radii of curvature. For the full pleated liner, the principal radii of curvature are equal and expressed by

$$R_1 = R_2 = \frac{\frac{D_T \sin\theta}{N_P}}{2\left(\tan\frac{\theta_P}{2} + \sec\frac{\theta_P}{2}\right)} \tag{5}$$

CR19

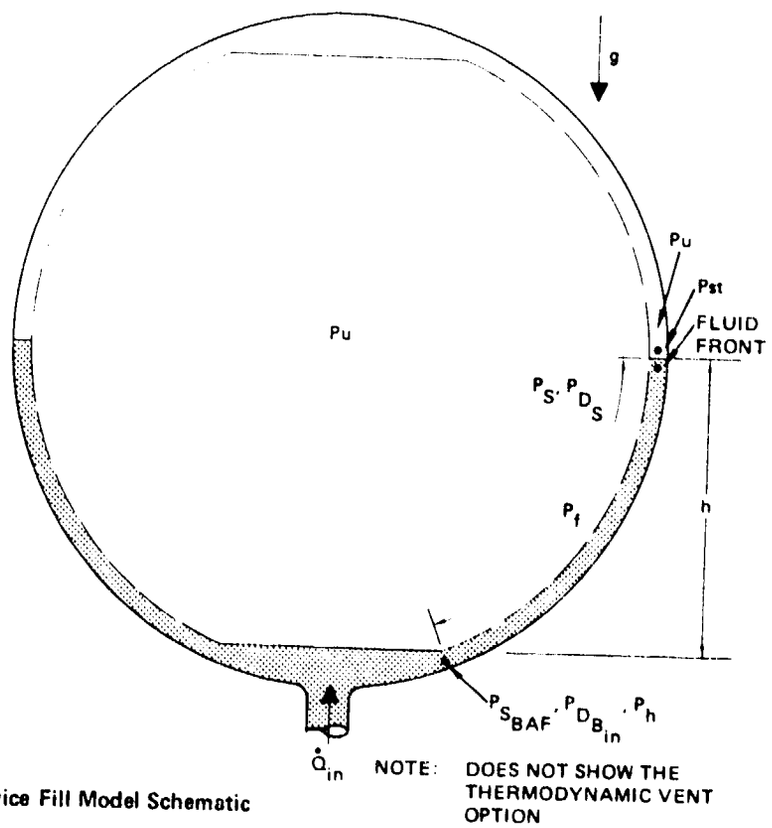

Figure 6. Screen Device Fill Model Schematic

For the channel configuration, the principal radii of curvature are one-half the base and one-half the height of the channel. Calculations (see Table 3) have shown that for low flow rates in a low 'g' environment (10^{-4} to 10^{-6} g's), the screen device will be completely filled or wicked over before flow through the screen (and into the tank) starts because the maximum static pressure in the screen device, which occurs at the inlet to the screen surface, is less than the ullage pressure.

The maximum static pressure inside the screen device is determined as follows:

$$P_{S_{BAF}} = P_U - P_{ST} + P_h + P_f - P_{D_{B_{in}}} + P_{D_S} \qquad (6)$$

The dynamic pressure and head pressure are

$$P_D = \frac{1}{2} \rho V^2 \qquad (7)$$

and

$$P_h = \rho ah \qquad (8)$$

The frictional pressure loss (P_f) is discussed under subroutines FRCTIØN and FRCTNC.

SUBROUTINE FLØWT

Subroutine FLØWT calculates the flow distribution for the full pleated liner configuration after the screen device is completely filled. The calculation is made for a specified time increment, Δt, or a specified slug of fluid, $VOL_{in} = \dot{Q}_{in} \Delta t$. The model assumes a pseudo-steady-state analysis and computes conditions along the screen device at an incremental angle, $\Delta\theta$.

Table 3

TYPICAL PRESSURE DISTRIBUTION IN THE SCREEN DEVICE

VARIABLE	FULL PLEATED LINER		MULTIARM SCREEN CHANNEL	
	N/m^2	(psi)	N/m^2	(psi)
ULLAGE PRESSURE (P_U)	413700	(60)	413700	(60)
STATIC PRESSURE AT THE SCREEN INLET ($P_{S_{BAF}}$)	413697	(59.99956)	413699.8	(59.99997)
CAPILLARY PRESSURE (P_{ST})	3.75	(5.44×10^{-4})	0.347	(5.03×10^{-5})
HEAD PRESSURE AT THE SCREEN INLET (P_h)	0.063	(9.15×10^{-6})	0.063	(9.15×10^{-6})
SCREEN FRICTIONAL PRESSURE LOSS (P_f)	0.216	(3.14×10^{-5})	0.056	(8.14×10^{-6})
DYNAMIC PRESSURE AT THE SCREEN INLET ($P_{D_{B_{in}}}$)	0.061	(8.81×10^{-6})	0.060	(8.75×10^{-6})
DYNAMIC PRESSURE AT THE FLUID FRONT (P_{D_S})	0.061	(8.81×10^{-6})	0.060	(8.75×10^{-6})

NOTES:

1. LIQUID PROPERTIES:
   SATURATED LH_2 @413700 N/m^2 (60 psia)
2. INFLOW RATE (~24-hr FILL)
   $\dot{Q}_{in} = 7.08 \times 10^{-6}$ m^3/sec (2.5×10^{-4} ft^3/sec)
3. LOCAL ACCELERATION:
   $g = 10^{-4}$ g's
4. FLUID FRONT LOCATION AT OUTLET BAFFLE

The model assumes a constant inflow rate and, for a given inlet static pressure (from subroutine FCNTL), computes the flow and pressure distribution.

The flow model is shown in Figure 7. The given variables are the system geometry, pipe inlet flowrate, and an initial guess for the pipe inlet static pressure. The conditions at the pipe inlet are calculated as follows:

$$P_{D_{in}} = \frac{1}{2} \rho V_{in}^2 \tag{9}$$

where

$$V_{in} = \frac{\dot{Q}_{in} + \dot{Q}_v}{A_{in}} \tag{10}$$

$$A_{in} = \frac{\pi}{4} D_i^2 \tag{11}$$

$$P_h = \rho a h_{in} \tag{12}$$

The baffle frictional pressure loss is determined as follows:

$$P_{f_B} = f \frac{\pi D_\Gamma \theta_{Bin}}{2S} \frac{1}{2} \rho V_B^2 \tag{13}$$

where

$$f = \frac{96}{R_{e_B}} \quad \text{for } R_{e_B} \leq 2000 \tag{14}$$

or

$$f = \frac{0.3636}{R_{e_B}^{0.2664}} \quad \text{for } R_{e_B} > 2000 \tag{15}$$

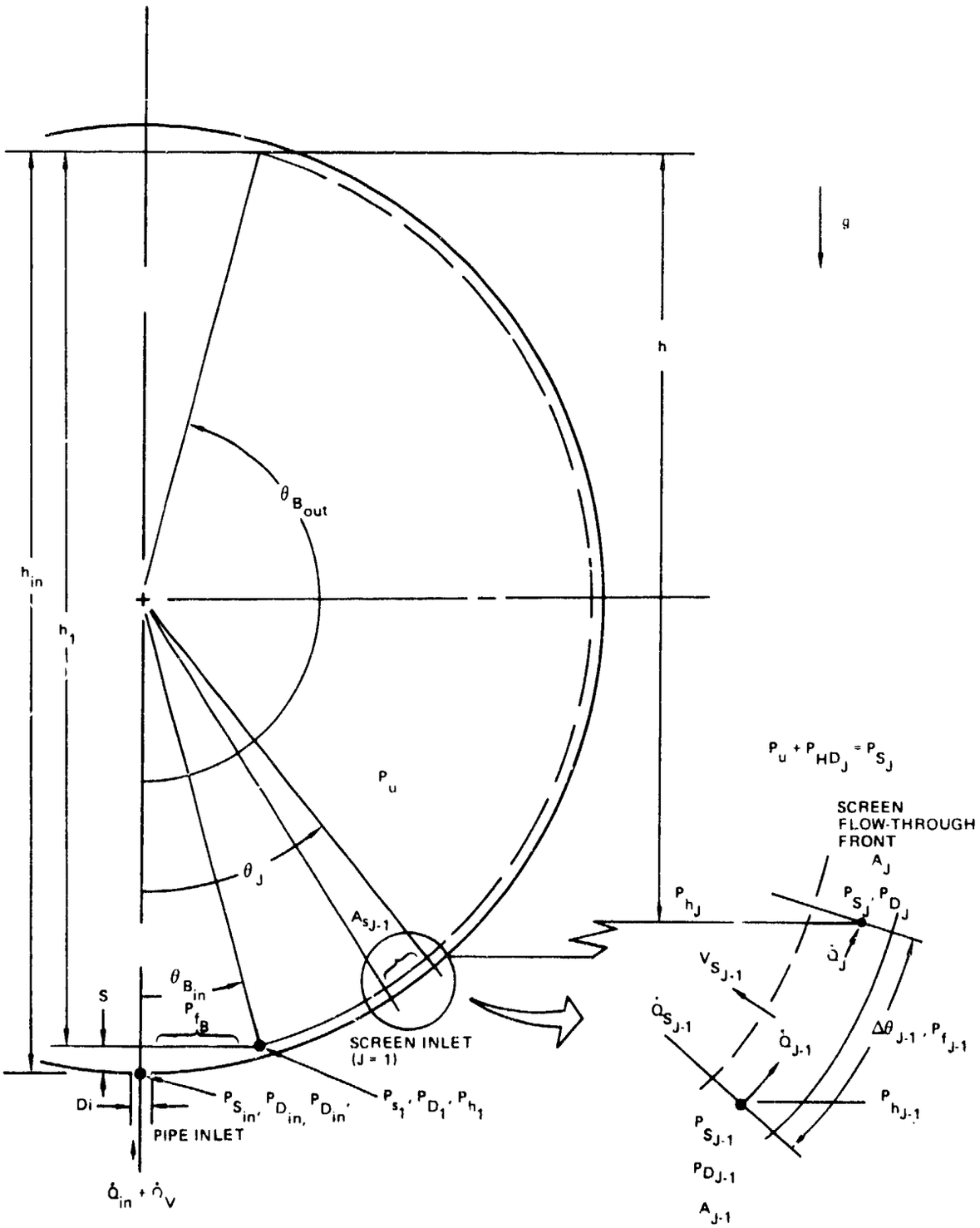

Figure 7. Flow Model Schematic

$$R_{e_B} = \frac{\rho V_B 2S}{\mu} \tag{16}$$

and

$$V_B = \frac{\dot{Q}_{in}}{\pi D_T S \sin\left(\frac{\theta B_{in}}{2}\right)} \tag{17}$$

The conditions at the screen inlet are calculated as follows:

$$V_1 = \frac{\dot{Q}_1}{A_1} \tag{19}$$

where

$$A_1 = \pi S D_T \sin \theta_{B_{in}} \tag{19}$$

$$\dot{Q}_1 = \dot{Q}_{in} \tag{20}$$

$$P_{D_1} = \frac{1}{2} \rho V_1^2 \tag{21}$$

$$h_1 = \frac{D_T}{2}\left(\cos \theta_{B_{in}} - \cos \theta_{B_{out}}\right) \tag{22}$$

$$P_{h_1} = \rho a h_1 \tag{23}$$

$$P_{S_1} = P_{S_{in}} + P_{D_{in}} + P_{h_{in}} - P_{D_1} - P_{h_1} - P_{f_B} \tag{24}$$

Once the screen inlet conditions are known, the pressures and flowrates in the screen segment, $\Delta\theta_1$, can be calculated. The generalized equations and the methodology are as follows (refer to Figures 7 and 8):

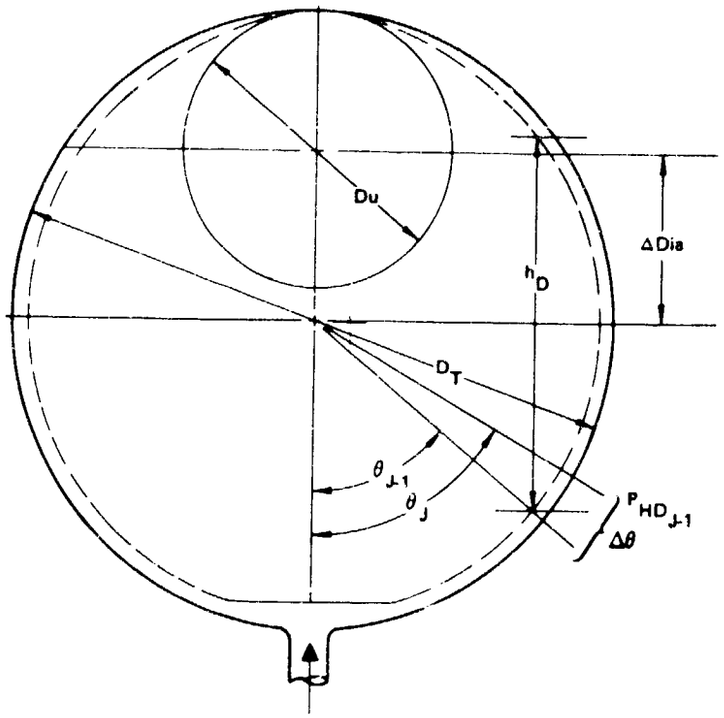

Figure 8. Schematic of Liquid Head Pressure on the Downstream Side of the Screen

A. Assuming the static pressure in the entire screen segment is constant at the inlet value, $P_{S_{J-1}}$, the approach velocity to the screen can be determined as follows:

$$V_{S_{J-1}} = \frac{\sqrt{A^2 + 4B\left(P_{S_{J-1}} - P_U - P_{HD_{J-1}}\right)} - A}{2B} \qquad (25)$$

where A and B are experimentally determined constants for the screen per Reference 1 and $P_{HD_{J-1}}$ is the liquid head pressure on the down stream side of the screen determined as follows (see Figure 8).

$$P_{HD_{J-1}} = \rho a h_D \qquad (26)$$

where

for $\theta_{J-1} < \pi/2$

$$h_D = \frac{D_T}{2} \cos \theta_{J-1} + \Delta dia \quad \text{if } D_u > D_t \sin \theta_{J-1} \tag{27}$$

$$h_D = D_T \cos \theta_{J-1} \quad \text{if } D_u \leq D_T \sin \theta_{J-1} \tag{28}$$

and for

$$\theta_{J-1} \geq \pi/2 \tag{29}$$

$$h_D = 0$$

B. The screen surface area for the screen segment is:

$$A_{S_{J-1}} = S_1 D_T N_P \Delta\theta_{J-1} \tag{30}$$

C. The flowrate through the screen is

$$\dot{Q}_{S_{J-1}} = V_{S_{J-1}} A_{S_{J-1}} \tag{31}$$

At this point, the volume of fluid which has flowed into the tank is summed, $VOL_T \sum_{i=1}^{J-1} \dot{Q}_{S_i} \Delta t$ and compared to the volume of fluid which has flowed into the system, $VOL_{in} = \dot{Q}_{in} \Delta t$. If VOL_T is less than VOL_{in}, then proceed to the next step. If VOL_T equals or exceeds VOL_{in}, the screen flow-through front has been reached. If VOL_T is greater than VOL_{in}, then the screen flow-through front angle (location) is determined as follows:

$$\Delta VOL_{T_{LAST}} = VOL_{in} - \sum_{i=1}^{J-2} \dot{Q}_{S_i} \Delta t \tag{32}$$

$$A_{S_{J-1}} = \frac{\Delta VOL_{T_{LAST}}}{V_{S_{J-1}} \Delta t} \tag{33}$$

$$\theta_J = \theta_{J-1} + \frac{A_{S_{J-1}}}{S_1 D_T N_P} \tag{34}$$

D. The flowrate to the next screen segment is

$$\dot{Q}_J = \dot{Q}_{J-1} - \dot{Q}_{S_{J-1}} \tag{35}$$

E. Assuming the flow along the screen segment is equal to the inlet flow, $\dot{Q}_{J-1}$, the frictional pressure loss ($P_{f_{J-1}}$) along the screen device is calculated in Subroutine FRCTIØN. Refer to the section on Subroutine FRCTIØN for a discussion of the model.

F. Next, the head pressure and dynamic pressure at the downstream end of the screen segment is determined as follows:

$$h_J = \frac{D_T}{2} \left(\cos \theta_J - \cos \theta_{Bow}\right) \tag{36}$$

$$P_{h_J} = \rho a h_J \tag{37}$$

$$A_J = \frac{D_T}{2} S_1 \sin \theta_J \sqrt{1 - \left(\frac{\pi D_T}{2 N_P S_1} \sin \theta_J\right)^2} \tag{38}$$

$$V_J = \dot{Q}_J / A_J \tag{39}$$

$$P_{D_J} = P_{D_{J-1}} \left(\frac{\dot{Q}_J}{\dot{Q}_{J-1}} \times \frac{A_{J-1}}{A_J}\right)^2 = P_{D_{J-1}} \left(\frac{V_J}{V_{J-1}}\right)^2 \tag{40}$$

G. Finally, the static pressure at the downstream end of the screen segment is determined as follows:

$$P_{S_J} = P_{S_{J-1}} + P_{D_{J-1}} + P_{h_{J-1}} - P_{D_J} - P_{h_J} - P_{f_{J-1}} \tag{41}$$

At this point, the static pressure, P_{S_J}, is compared with the required static pressure, $P_U + P_{HD_J}$. If P_{S_J} is less than $P_U + P_{HD_J}$, program control is returned to subroutine FCNTL where $P_{S_{in}}$ is adjusted. This comparison is made at the end of each angular incrementation to assure that fluid can be passed through the screen if the screen flow-through fluid front has not been reached. If the screen flow-through front is reached (see step C.), program control is returned to subroutine FCNTL to determine if pressure convergence has been attained.

SUBROUTINE FLØWTC

Subroutine FLØWTC calculates the flow distribution for the multiarm screen channel configuration after the screen device is completely filled. The assumptions and methodology are identical to those discussed in the section on Subroutine FLØWT except for the difference in the screen flow-through area as a function of angle from the vertical, the screen device cross-sectional area, and the methodology to determine the head pressure on the downstream side of the screen.

The screen device cross-sectional area is constant and is equal to the base times the height of the channel.

The screen flow-through area is

$$A_S = 2 N_P N_C \frac{H_P}{\cos \theta_P} \left(D_S \Delta \theta \right) \tag{42}$$

but between the screen windows, the screen flow-through area is zero. Subroutine GEØMTRY computes the total screen area from the inlet baffle to the outlet baffle in increments of $\Delta\theta$. Thus, subroutine FLØWTC applies a linear interpolation (FUNCTION BETA) to obtain the screen area as a function of θ_J.

Because the liquid is assumed to be contained in the gap between the screen device and tank wall (see Figure 1), the liquid head is the distance from the top of the liquid to the point of interest.

SUBROUTINE FRCTIØN

Subroutine FRCTIØN calculates the frictional pressure loss in the full pleated liner between two angles for a specified flowrate. The equation is derived in Reference 2, Appendix D. In this derivation, the cosine of the pleat half-angle was assumed constant at 0.93 because it only varied from 0.9922 (cos 7.18 deg) and 0.866 (cos 30 deg). The equation is:

$$P_f = \left[\frac{a}{2} \left(\frac{\sin \theta_2}{\cos^2 \theta_2} + \frac{\sin \theta_1}{\cos^2 \theta_1} \right) + \left(\frac{a}{2} + b \right) \left(\tan \theta_2 + \tan \theta_1 \right) + c \ell n \frac{\tan \frac{\theta_2 + \frac{\pi}{2}}{2}}{\tan \frac{\frac{\pi}{2} - \theta_1}{2}} \right] \rho \tag{43}$$

where

$$a = \frac{53 \mu}{2 \rho} \frac{N^2 \dot{Q}}{0.93^3 \pi^2 S_1 D^2} + \frac{N \dot{Q}^2}{4(6.6046)\ 0.93^3 \pi^3 D^2 S_1^2} \tag{44}$$

$$b = \frac{53 \mu}{2 \rho} \frac{N \dot{Q}}{0.93^3 \pi^2 D S_1^2} + \frac{\dot{Q}^2}{8(6.6046)\ 0.93^3 \pi^2 D S_1^3} \tag{45}$$

$$c = \frac{53 \mu}{8 \rho} \frac{\dot{Q}}{0.93^3 \pi S_1^3} \tag{46}$$

SUBROUTINE FRCTNC

Subroutine FRCTNC calculates the frictional pressure loss in the screen channel configuration between two angles for a specified flowrate. The equation is derived in Reference 1, pages 43-55. The equation is:

$$P_f = f \frac{\rho L_s}{2 D_h} V^2 \tag{47}$$

where

$$f = \frac{96}{R_e} + \frac{1}{4\left(\log \frac{3.7}{\epsilon / D_h}\right)^2} \tag{48}$$

$$R_e = \frac{\rho V D_h}{\mu} \tag{49}$$

and

$$D_h = \frac{4 \times \text{Area}}{\text{Wetted Perimeter}} \tag{50}$$

Because the channel consists of screen and smooth metal, a weighted average value was computed for the friction factor. Furthermore, since the screen windows are much larger than the metal supports between them, the difference in pressure losses was neglected and the computation was made assuming screen surface along the entire length of the channel.

SUBROUTINE GEØMTRY

Subroutine GEØMTRY calculates, for the full pleated linear and screen channel configurations: the height above the baffle, the volume inside the screen device, the volume outside the screen device, the screen surface area, the cross-sectional area inside the screen device, and the cross-sectional area in the tank (excluding the screen device) as a function of angle from the vertical (refer to Figures 9 and 10).

The height above the baffle is:

$$h_l = \frac{D_T}{2} \left(\cos \theta_{B_{in}} - \cos \theta\right) \tag{51}$$

where θ is the angle of interest.

The total tank cross-sectional area is:

$$A_O = \left(\frac{D_T}{2} \sin \theta\right)^2 \tag{52}$$

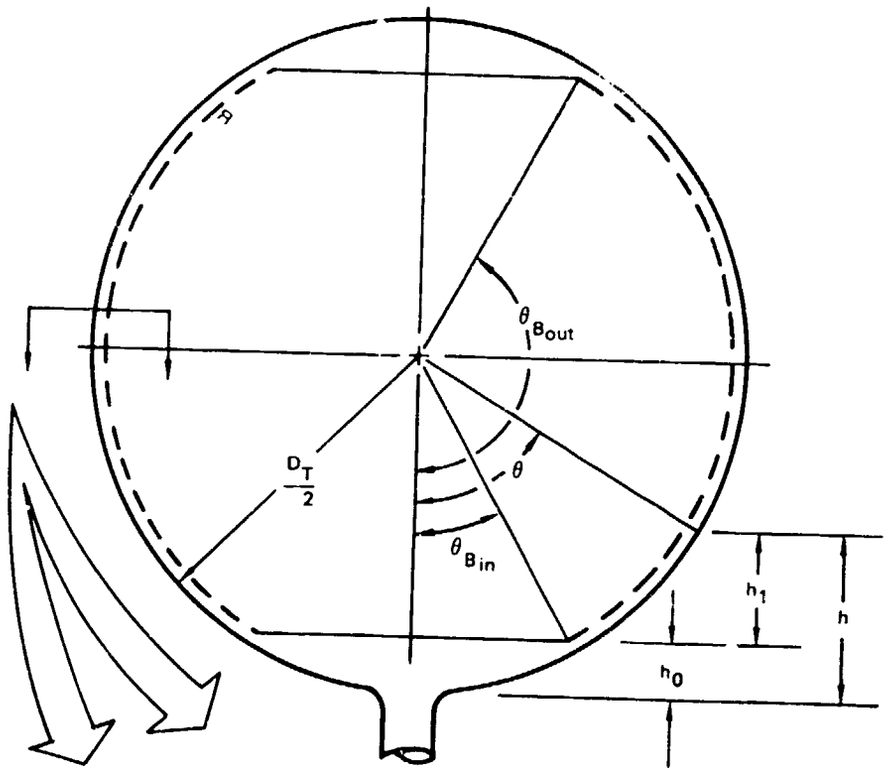

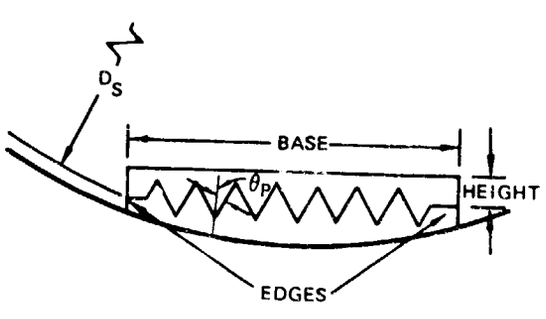

MULTIARM SCREEN CHANNEL

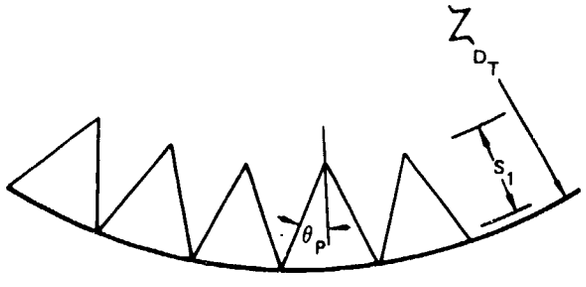

FULL PLEATED LINER

Figure 9. Schematic of System Geometry

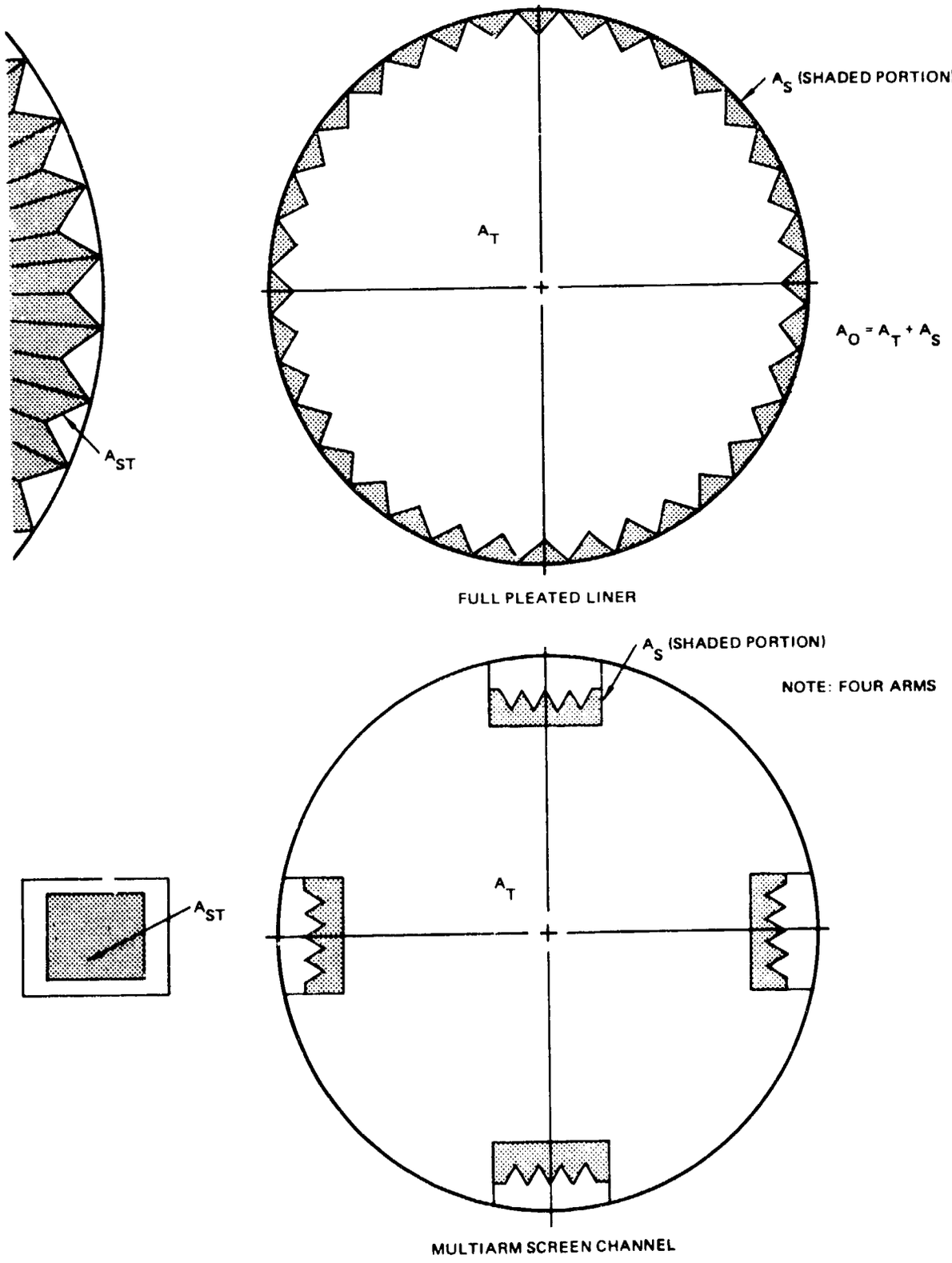

Figure 10. Schematic of System Areas

The cross-sectional area inside the screen device is:

$$A_S = S_1^2 N_P \sin(2\theta_P) \qquad \text{(pleated liner)} \tag{53}$$

$$A_S = \text{Base} \times \text{ht} \times N_C \qquad \text{(screen channel)} \tag{54}$$

Therefore, the cross-sectional area inside the tank including the screen device is:

$$A_T = A_0 - A_S \tag{55}$$

The total tank volume above the inlet baffle as a function of height (or angle) is:

$$V_0 = \frac{\pi}{3}\left(h^2\left(3\frac{D_T}{2} - h\right) - h_O^2\left(3\frac{D_T}{2} - h_O\right)\right) \tag{56}$$

where h_O is the baffle height and h is the height from the bottom of the tank. The volume inside the screen device is:

A. Pleated liner

$$V_S = \pi\left(\frac{D_T}{2}\right)^2 S_1\left[-\frac{1}{2}\cos\theta\sqrt{1-\left(\frac{\pi D_T}{2S_1N_P}\sin\theta\right)^2} - \frac{1-\left(\frac{\pi D_T}{2S_1N_P}\right)^2}{2\frac{\pi DT}{2S_1N_P}}\right.$$

$$\left.\log\left(\frac{\pi D_T}{2S_1N_P}\cos\theta + \sqrt{1-\left(\frac{\pi D_T}{2S_1N_P}\sin\theta\right)^2}\right)\right]_{\theta=\theta_{B_{in}}}^{\theta=\theta} \tag{57}$$

B. Screen channel

$$V_S = A_S D_S \left(\theta - \theta_{B_{in}}\right) \tag{58}$$

Therefore, the volume outside the screen device is:

$$V_T = V_0 - V_S \tag{59}$$

The screen surface area as a function of θ is:

A. Pleated liner

$$A_{S_T} = 2 S_l N_P D_T \left(\theta - \theta_{B_{in}}\right) \tag{60}$$

B. Screen channel

$$A_{S_T} = 2 N_P \frac{h_p}{\cos \theta_p} D_S \sum \theta_S N_C \tag{61}$$

where $\Sigma \theta_S$ is the sum of the screen window angles as a function of θ. Therefore, it excludes the support structure between the screen windows.

SUBROUTINE INDATA

Subroutine INDATA is the data input routine which initializes and computes some variables, prints out the input data, and converts the metric input data to English units for use in the remainder of the math model.

The data are inputed by the Fortran READ statement. The input data are grouped according to their use with each group preceded by a descriptive card containing an integer, in card columns 1 and 2, and a description of the data in the other card columns. Because the format is I2, the description is not read. The card is followed by one or more specialized cards that contain the data.

SUBROUTINE INTERP

Subroutine INTERP is a second-order interpolation routine. The basic equation is:

$$U = aV^2 + bV + c \tag{62}$$

The constants a, b, and c are obtained from the simultaneous solution of three second order equations as follows:

$$\begin{aligned} y_{J-1} &= a\,x_{J-1}^2 + b\,x_{J-1} + c \\ y_J &= a\,x_J^2 + b\,x_J + c \\ y_{J+1} &= a\,x_{J+1}^2 + b\,x_{J+1} + c \end{aligned} \tag{63}$$

SUBROUTINE STBLTY

Subroutine STBLTY determines the liquid-vapor interface stability for three different system flows: flow into the system, the screen device, and through the screen device into the tank. The liquid-vapor interface stability is characterized by the Weber number

$$W_e = \frac{\rho V^2 L}{\sigma} \tag{64}$$

where L is the characteristic length and V is the characteristic flow velocity. The three characteristic Weber numbers become increasingly more restrictive for the three flows considered.

For the flow into the system, the characteristic length is the inlet line radiu and the characteristic velocity is the average inlet flow velocity or

$$W_e = \frac{\rho V_{in}^2 D_{in/2}}{\sigma} \tag{65}$$

Considerable work has been accomplished by NASA LeRC in developing correlations for liquid-vapor interface stability criteria for flow into various kinds of tanks (Reference 9 to 14) but none has been done with flow into a screen device. The Weber number stability criterion for an unbaffled tank has been shown to be 1.5 (Reference 12).

The comparison of different types of baffle configurations (Figure 11 taken from Reference 14) indicated that the Weber number could be increased by 4 to 120 times depending on the type of baffle used. Therefore, depending on the choice of baffle used to approximate the full pleated liner or multiarm screen channel, the inflow Weber number stability criteria can vary from 1.5 to 180. The critical Weber number is an input to the math model. The value computed from Equation (65) is compared with the input value and, if it is exceeded, the run is terminated. For this study, it was assumed that the full pleated liner and multiarm screen channel could be approximated by the stacked disc configuration because of the effects of the screen in aiding stability, thus the critical Weber number for stable flow into the system was assumed as 84.

For flow in the screen device, the characteristic length is the hydraulic radius of the flow cross-section defined by

$$R_h = \frac{2 \times \text{Area}}{\text{Perimeter}} \tag{66}$$

and the characteristic velocity is the average flow velocity of the fluid front. The math model computes the Weber number of the fluid front for each time increment during the screen device filling and assumes that a stable liquid-vapor interface exists if the surface tension forces are greater than the inertial forces or the Weber number is less than one. A larger value could be possible but requires experimental verification.

The stability of the flow into the main tank is more complex. For the pleated liner, the liquid will be weeping through the screen, thus the stability criterion was based on the Weber number, with the radius from tank center to screen being the characteristic length. The flow velocity will be different through each screen segment; thus, for conservation, the stability criterion was applied to the largest value of flow velocity.

For the screen channel configuration, the flow into the main tank is even more complex. Referring to Figure 12, the liquid will first flow into the channel (1), then through the screen into the space between the channel and tank wall (2), then through the side of the channel into the main tank (3). The flow into the main tank will then merge with the flow from the adjacent screen channel and flow toward the center of the tank (4). Due to this complex flow, the tank radius was assumed to be the characteristic length.

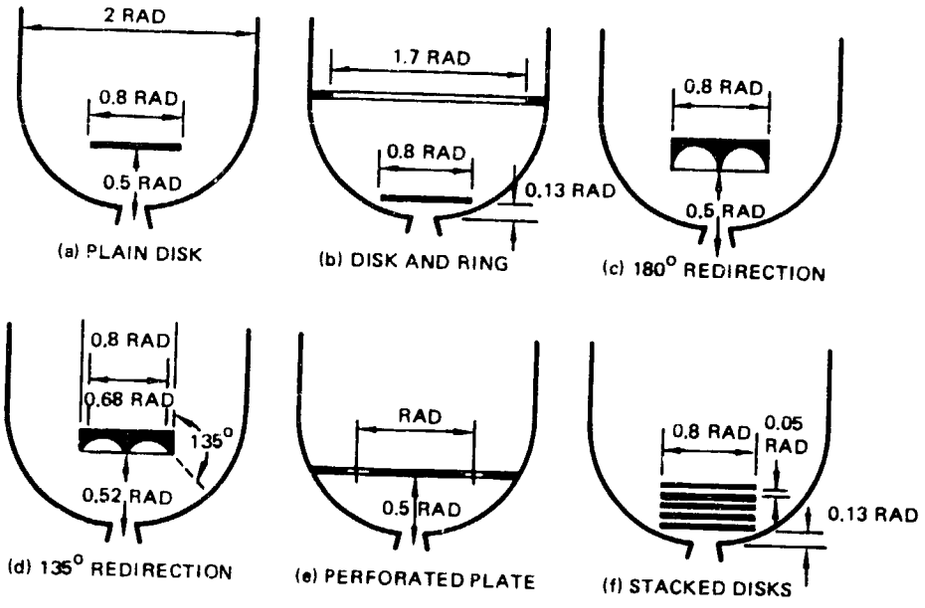

INFLOW BAFFLE CROSS SECTIONS

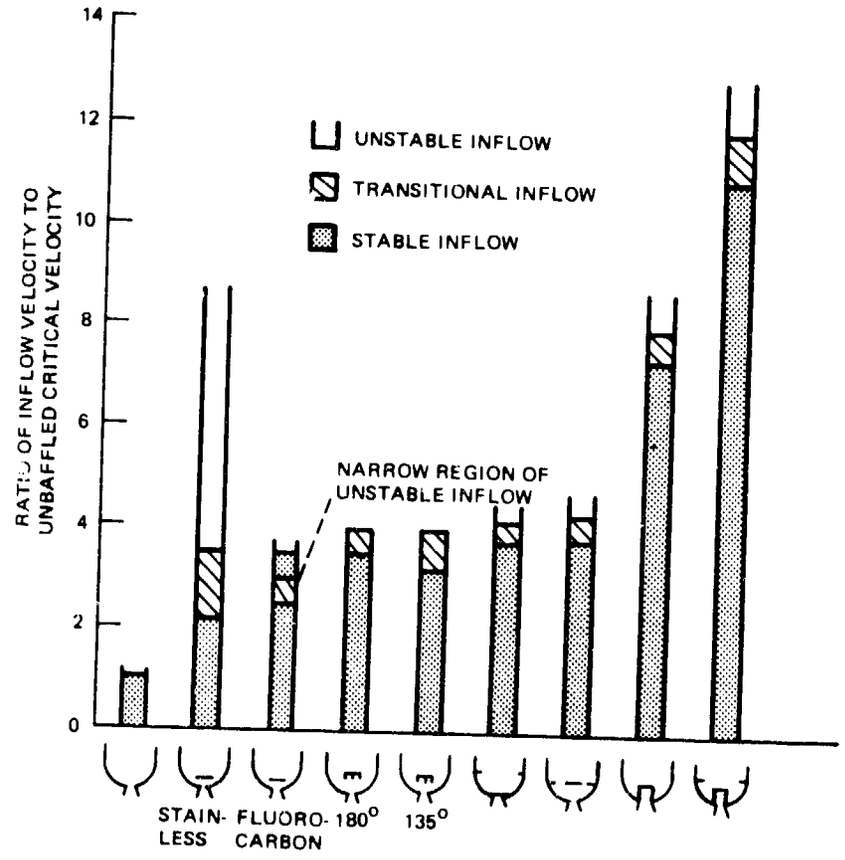

COMPARISON OF INFLOW BAFFLE EFFECTIVENESS

Figure 11. Baffle Configuration and Effectiveness

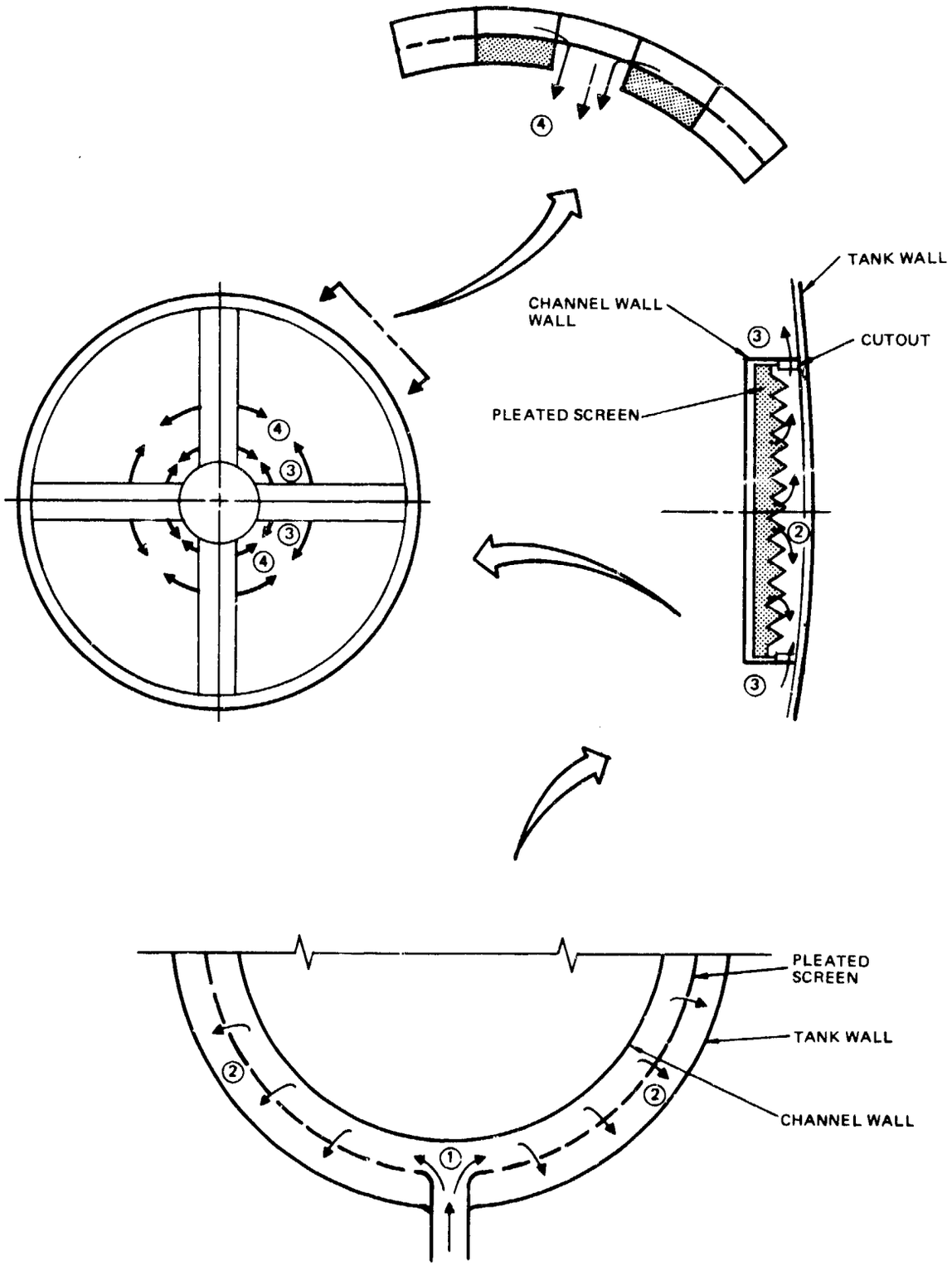

Figure 12. Screen Channel Configuration Flow Schematic

The largest flow velocity (and Weber number) will occur at the inlet to the screen device for a positive 'g' field, because the differential pressure across the screen is the greatest at this point. The math model computes and compares the liquid-vapor interface stability only for the first slug of liquid through the screen because each succeeding slug of liquid should yield approximately the same Weber number. The math model assumes that a stable liquid-vapor interface exists if the surface tension forces are greater than the inertial forces or the Weber number is less than one.

The inlet flow velocities (or fill rates) to satisfy the three criteria described above differ by more than four orders-of-magnitude (for the Spacelab tank) and it is not clear which criterion should be governing. This is discussed in detail below in the section on Operational Aspects.

SUBROUTINE TNKFLL

Subroutine TNKFLL calculates the liquid and ullage geometry in the tank as the liquid flows through the screen for a stable liquid-vapor interface. The analysis consists of two parts. The first part determines the forming of the ullage bubble and the second part computes the geometry after the ullage bubble has been formed.

Calculations (see Subroutine FLØWF) have indicated that in a low-g environment (10^{-4} to 10^{-6} g's) the screen device will be completely filled before the liquid flows through the screen. As the liquid flows through the screen the ullage bubble assumes a spherical shape because this shape yields the minimum energy across the liquid-vapor interface.

Since the process of forming the ullage bubble is not germane to this analysis and cannot be readily determined due to the complexity of the screen device and lack of test data, a simplified approach was taken. For the full pleated liner, the model assumes that the pleats are filled first (see Figure 9) and once the pleats are filled the ullage bubble is formed. This is not exactly correct because of the upper baffle (see Figure 9), but this assumption yields an approximate time to form the ullage bubble. The assumption, that the pleats are filled first, is justified because of the very small flow velocities

through the screen and the surface tension forces that will tend to keep the liquid in the vicinity of the pleated liner. Since the full pleated liner is symmetrical about its centerline (see Figure 9), the expression for the volume of the pleated liner to be filled is identical to equation (57).

For the multiarm screen channel system, the liquid is assumed to fill the void between the channel and the tank wall first (see Figure 9). The volume is expressed by

$$V_{F_{MAX}} = \text{Base} \times H_{ST} (\theta_{B_{out}} - \theta_{B_{in}}) N_C \tag{67}$$

Calculations have indicated that the surface tension forces for the channel slits are greater than the head pressure in low-g (10^{-4} to 10^{-6} g's), therefore, the assumption that the void is filled first is justified. The model further assumes that once this void is filled, the ullage bubble has been formed. Although this is not correct, a specific model would require test data. Since the process of forming the ullage bubble is not germane to this analysis, the computed time is useful in knowing when the void is filled.

Once the ullage bubble has been formed, the model assumes that the bubble is attached to the top of the tank (see Figure 13). The ullage volume is computed as

$$V_U = V_T - V_{liq} \tag{68}$$

and the ullage diameter is

$$D_U = \left(\frac{6}{\pi} V_U\right)^{1/3} \tag{69}$$

As more liquid flows into the tank, the ullage volume and diameter continues to decrease until the desired fill ratio (V_U/V_t) is attained. The desired fill ratio is an input to the math model but the actual fill ratio (or volume) will depend on the location of the vent line if the system is being vented during fill or if the maximum allowable ullage pressure for an unvented tank is reached.

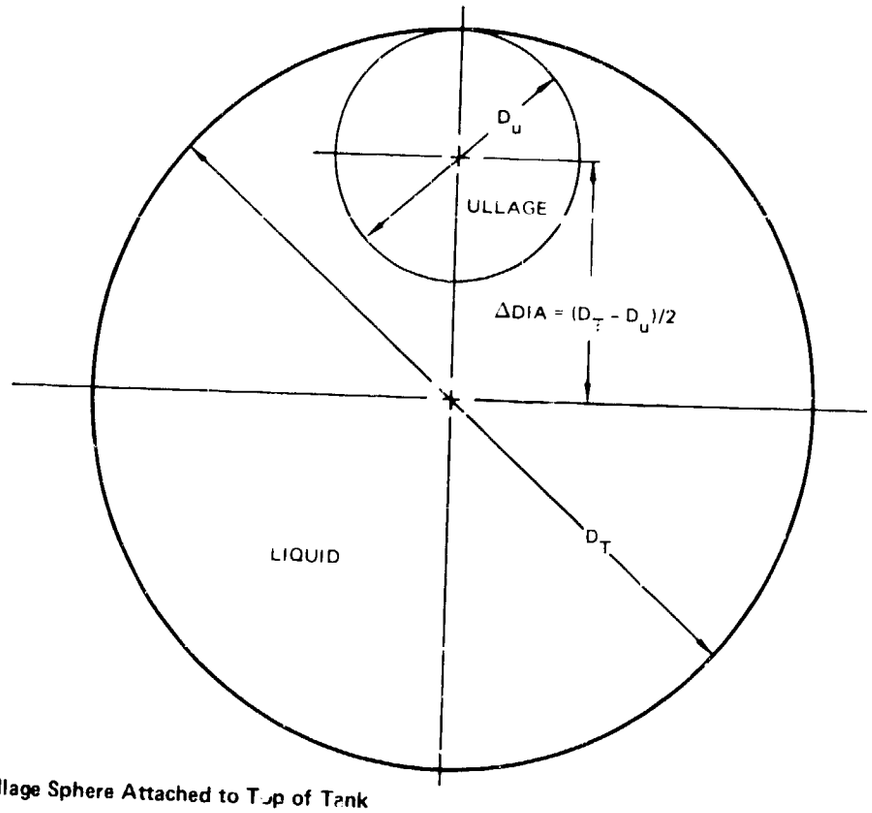

Figure 13. Ullage Sphere Attached to Top of Tank

The assumption that the ullage bubble is spherical is justified because of the small Bond number in the low-g (10^{-4} to 10^{-6} g's) environment. The Bond number for the fluids considered in this study are shown in Table 4. A NASA study (Reference 15) substantiates the near-spherical shape of the ullage bubble for most of these Bond numbers.

SUBROUTINE ULLAGE

Subroutine ULLAGE calculates the ullage conditions (pressure, temperature and mass) and the vent flow requirements during filling. The model provides for a two-component ullage that consists of a pressurizing gas and liquid vapors. The three available options are:

1. Constant pressure and temperature
2. Compression with no heat or mass transfer
3. Ullage vapor condensation by a thermodynamic vent

The constant pressure and temperature case assumes that the ullage gas is vented to maintain the constant pressure. The vent flowrate is calculated, thus the required vent size can be determined.

Table 4

BOND NUMBER AS A FUNCTION OF THE LOCAL ACCELERATION

Local Acceleration (g's)	Fluid			
	LH_2	LO_2	MMH	N_2O_4
1.0	170,000	312,000	70,000	150,000
10^{-4}	17.0	31.2	7.0	15.0
10^{-5}	1.7	3.12	0.7	1.5
10^{-6}	0.17	0.312	0.07	0.15

NOTES:

1. LH_2 properties at 413,700 N/m^2 (60 psia) saturation
2. LO_2 properties at 413,700 N/m^2 (60 psia) saturation
3. MMH properties at 293.3 K (528 deg R)
4. N_2O_4 properties at 293.3 K (528 deg R)

The compression assumes no heat or mass exchange between the ullage, liquid and surrounding, and the ullage pressure is held constant over each time increment. The ullage temperature is determined from the conservation of energy and mass considerations and is expressed by

$$T_{u_2} = T_{u_1} - \frac{P_{u_1} \Delta V_u}{W_u C_{v_u} + W_{u_{pg}} C_{v_{pg}}} \tag{70}$$

The new ullage pressure can then be calculated from the perfect gas equation as

$$P_{u_2} = \left(W_u R_u + W_{u_{pg}} R_{u_{pg}} \right) \frac{T_{u_2}}{V_{u_2}} \tag{71}$$

The constant pressure for each time increment assumption requires that the change in pressure over each time increment be small.

The computation will terminate if the ullage pressure exceeds an input maximum value ($P_{u_{max}}$).

The thermodynamic fill-vent model is schematically depicted in Figure 14. The system operates by supplying liquid, directly from the incoming flow, to the thermodynamic fill-vent viscojet. The liquid is expanded to a lower pressure and temperature in the vent line then boils in the vent line by extracting heat from and condensing the ullage gas. A two-component ullage is assumed but the pressurizing gas is assumed to have a lower condensation temperature than the vapor and none of it condenses. The condensation process is g-dependent in the sense that the condensation heat transfer coefficient depends on the thickness of the condensate liquid film. This analysis assumes that surface tension forces remove the film in low-g. The effective length of the thermodynamic vent line is assumed to be equal to the portion exposed to the ullage bubble.

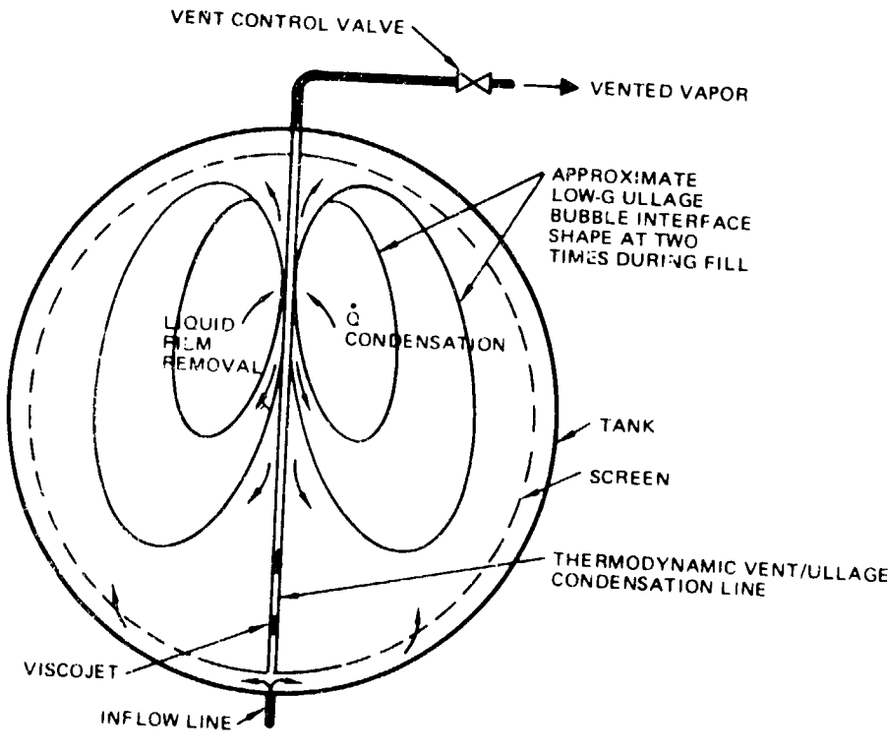

Figure 14. Interface/Liquid Film Effects on Thermodynamic Fill Vent

Figure 15 is a schematic of the heat transfer analysis. The thermal resistance between the ullage and thermodynamic vent-fluid consists of filmwise condensation on the outside of the vent line, conduction through the vent line wall, and boiling heat transfer for saturated fluids in convective flow inside the vent line.

CR19

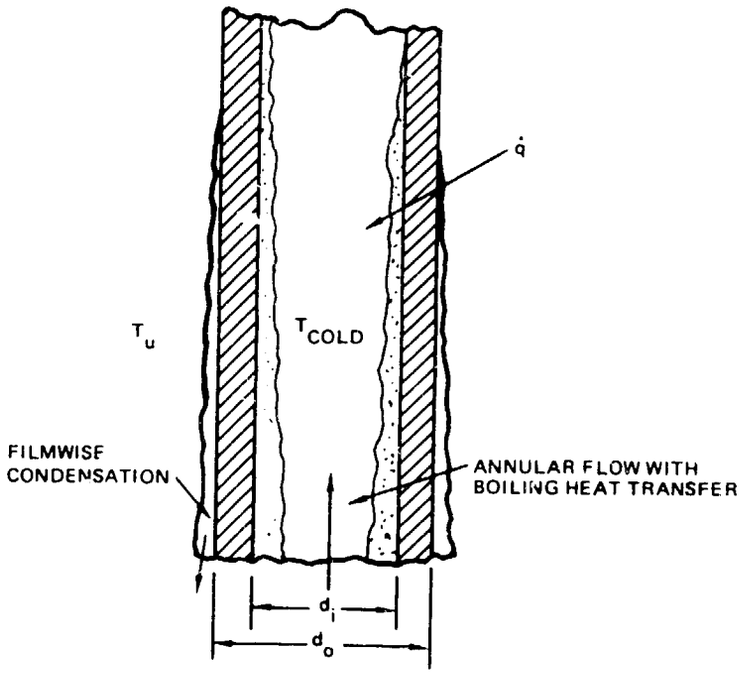

Figure 15. Heat Transfer Model

The thermal resistance on the inside of the vent line is

$$R_i = \frac{1}{d_i h_i} \tag{72}$$

where h_i is determined from the correlation of Chen for annular flow regime boiling as described in Reference 16. The correlation is

$$h_i = S\,(0.00122)\,\frac{k_L^{0.79}\,C_p^{0.45}\,\Delta T_i^{0.24}\,\Delta P_{sat}^{0.75}}{\sigma^{0.5}\,\mu_L^{0.29}\,h_{fg}^{0.24}\,\rho_v^{0.24}} + F\,(0.023)\,(Re)_L^{0.8}\,(Pr)_L^{0.4}\,\frac{k_L}{d_i} \tag{73}$$

where S and F are empirically determined dimensionless functions allowing for variations in the boiling and forced convection components. The value of S and F are given in Figures 16 and 17.

The thermal resistance through the vent line wall is

$$R_w = \frac{\ell n \left(\frac{d_o}{d_i}\right)}{2 k_w} \tag{74}$$

The thermal resistance on the outside of the vent line is

$$R_o = \frac{1}{d_o h_c} \tag{75}$$

where h_c is the heat transfer filmwise condensation coefficient

CR19

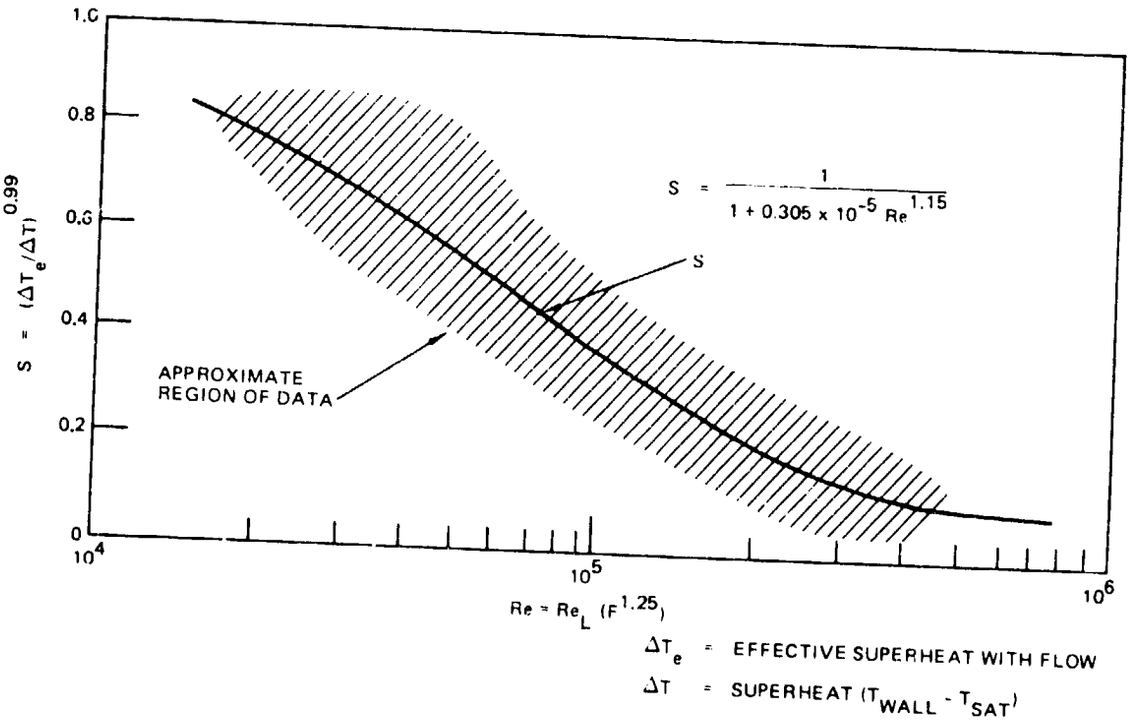

Figure 16. Suppression Factor, S

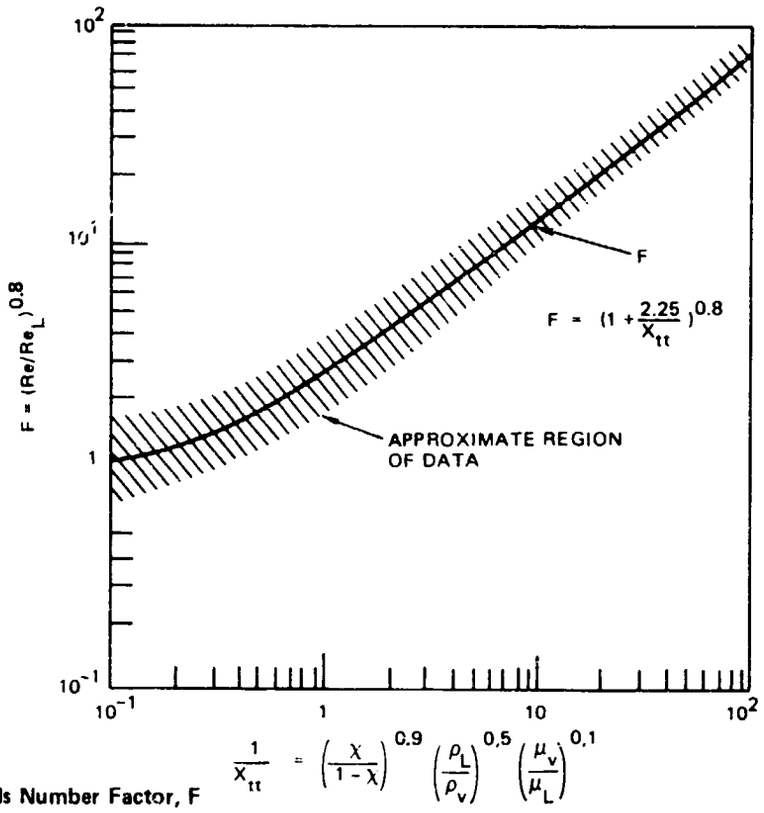

Figure 17. Reynolds Number Factor, F

$$h_c = 0.943 \left[\frac{\rho (\rho - \rho_v) \, h'_{fg} \, k_L^{\,3} \, a}{L_{HE} \, \mu_L \, \Delta T_o} \right]^{1/4} \tag{76}$$

where $h'_{fg} = h_{fg} + 3/8 \, C_p \, \Delta T_o$.

The total thermal resistance is

$$R_T = R_i + R_w + R_o \tag{77}$$

Since equations (73) and (76) had to use an assumed distribution of the temperature drop from the ullage to the vent fluid ($\Delta T = \Delta T_o + T_i$), the math model determines if the distribution was correct by comparing the thermal resistances which are directly proportional to the temperature drops. If the initial guess is not within a specified limit (RCØNVG), a new distribution is assumed and the heat transfer coefficients and thermal resistances are recomputed.

The overall heat transfer coefficient is the inverse of the thermal resistance

$$U_i d_i = \frac{1}{R_T} \tag{78}$$

The heat transfer rate is

$$\dot{q} = \pi U_i d_i L_{HE} \Delta T \tag{79}$$

The ullage mass condensed is

$$W_c = \frac{\dot{q}}{h_{fg}} \Delta t \quad E_{ff} \tag{80}$$

where E_{ff} is an efficiency factor that is included to allow the degradation of the heat exchange mechanism if future testing so indicates. This factor could be used if it is found that the flow in the thermodynamic vent line is in the mist flow regime instead of the assumed annular flow regime (Eq. 73), or the analysis could be revised to account for the appropriate flow regime. If the thermodynamic vent-line flow is in the mist flow regime the heat transfer coefficient could be reduced an order of magnitude from the annular flow regime value. Because the heat transfer coefficient for filmwise condensation on the outside of the vent line is an order of magnitude smaller than the annular flow heat transfer coefficient, the mist flow assumption would result in the heat transfer being reduced approximately by one-half.

The ullage temperature is determined from the conservation of energy and mass considerations. The resulting equation is:

$$T_{u_2} = T_{u_1} - \frac{\left(R_u T_{u_1} - H_{V_u}\right) W_c + \dot{q} \Delta t + P_{u_1} \Delta V_u}{W_{u_2} C_{V_u} + W_{u_{PG}} C_{V_{u_{PG}}}} \tag{81}$$

Finally, the pressure is calculated from the ideal gas equation

$$P_{u_2} = \left(W_{u_2} R_u + W_{u_{pg}} R_{u_{pg}} \right) \frac{T_{u_2}}{V_{u_2}} \tag{82}$$

SUBROUTINE WICK

Subroutine WICK determines the wicking distance and time at which wickover occurs, when the wicking front reaches the end of the screen device or outlet baffle (see Figure 1). Because the math model uses a time incrementation, the wicking time and angular location are determined by a second order interpolation of the last three computed wicking front radial distances relative to the inlet baffle.

The analytical model for the wicking velocity (or wicking distance) as a function of system parameters (liquid properties, gravitational environment, geometry) is found in Reference 17:

$$V_w = \frac{C_s}{L_w}\left(\frac{\sigma}{\mu}\right) - C_s\left(\frac{\rho a}{\mu}\right)\frac{D_p}{\phi}\sin\alpha \qquad (83)$$

Because the wicking velocity and distance have an inverse relationship for a non-zero liquid flow front (filling of screen device), the wicking velocity will be identical to the fluid front velocity, that is, the wicking distance and fluid front will be in equilibrium. All the liquid inflow is contained in the screen device (see Subroutine FLØWF) until the screen device is filled so the fluid advance velocity is expressed as

$$V_f = \frac{\dot{Q}_{in}}{A \sin\theta} \qquad (84)$$

where A is the flow cross-sectional area for either the full pleated liner or multiarm screen channel. These expressions are developed in Subroutine GEØMTRY as Equations (53) and (54). Once the wicking velocity is known, the wicking distance is determined from Equation (83).

SUBROUTINE ØUTDAT

Subroutine ØUTDAT writes out the computed data and the appropriate headings converting the variables from English units to metric units as required.

In addition to the output data written by subroutine ØUTDAT, the math model is also capable of writing out interim calculated values for pressures, flowrates, wicking velocity, etcetera depending on the value given to the input flag

IWRITE. The output values are written during the calling sequence to subroutines FCNTL, FLØWF, FLØWT, FLØWTC, GEØMTRY, TNKFLL, ULLAGE, and WICK.

FUNCTION BETA

Function BETA is a linear interpolation routine. The basic equation is:

$$\beta = Y_{J-1} + (Y_J - Y_{J-1}) \frac{\alpha - X_{J-1}}{X_J - X_{J-1}} \tag{85}$$

OPERATIONAL ASPECTS

Computer Program P 5762, Screen Device Filling Analysis, is operational on the MCAUTO CDC CYBER 74 computer system. Checkout cases have been run as functions of the fluid (LH_2, LO_2, MMH, and N_2O_4), screen acquisition device (multiarm screen channel and full pleated liner), inflow rates (6-, 12-, 24-, and 48-hr fill), system pressure, temperature, and gravitational environment (zero and low-g), as shown in Table 5. The description of "coils" and "coil dia" in Table 5 refers to the number of passes and the tube diameter of the TVS fill vent tubing heat exchanger. In addition, all the options listed in Table 1 have been tested, and the model appears to be fully operational. Some of the results determined from these limited checkout runs follow, and the pertinent data from a typical LH_2 run are shown in Table 6.

The screen wickover phenomenon is of importance during the filling of the screen device, but this analysis assumes that wicking is restricted to the screens. Due to the moving fluid front and the fill rates considered, the trapped gas volume so determined at wickover is small and insensitive to the gravitational environment. Table 7 shows some typical values. Additional wicking paths may occur within the corners of the channel or liner, so the values shown in Table 7 may be exceeded. One way to eliminate the trapped gas volume would be to withdraw the TVS fluid from the gas-filled end of the screen channel(s) or liner. Low-g testing should be conducted to determine the quantity of gas trapped, and elimination techniques.

Table 5

MATRIX OF CHECKOUT CASES

Fluid	Ullage Pressure N/m^2 (psia)	I_{type}*	t_{Fill}, hr	Screen Type*	g's	Coils	Coil Dia cm (in)
LH_2	413,700 (60)	CP	24	PL	10^{-6}	--	--
LH_2	413,700 (60)	CP	24	C	10^{-6}	--	--
LH_2	68,950 (10)	COMP	24	C	10^{-6}	--	--
LH_2	206,850 (30)	COMP	24	C	10^{-6}	--	--
LH_2	413,700 (60)	COMP	24	C	10^{-6}	--	--
LH_2	413,700 (60)	TVS	24	C	10^{-6}	2	0.64 (0.25)
LH_2	413,700 (60)	TVS	24	C	10^{-6}	4	0.64 (0.25)
LH_2	413,700 (60)	TVS	24	C	10^{-6}	10	0.64 (0.25)
LH_2	413,700 (60)	TVS	24	C	10^{-6}	1	0.64 (0.25)
LH_2	413,700 (60)	TVS	24	C	10^{-6}	1	0.64 (0.25)
LH_2	413,700 (60)	TVS	24	C	10^{-6}	1	1.27 (0.50)
LH_2	413,700 (60)	TVS	48	C	10^{-6}	1	1.27 (0.50)
LH_2	413,700 (60)	TVS	96	C	10^{-6}	1	1.27 (0.50)
LH_2	344,800 (50)	COMP	24	C	10^{-6}	--	--
LH_2	68,950 (10)	COMP	24	C	10^{-6}	--	--
LH_2	344,800 (50)	TVS	24	C	10^{-6}	1	0.64 (0.25)
LH_2	68,950 (10)	TVS	24	C	10^{-6}	1	0.64 (0.25)
LH_2	413,700 (60)	CP	24	C	0	--	--
LO_2	413,700 (60)	CP	24	C	10^{-6}	--	--
LO_2	413,700 (60)	TVS	24	C	10^{-6}	1	0.64 (0.25)
MMH	413,700 (60)	CP	24	C	10^{-6}	--	--
N_2O_4	413,700 (60)	CP	24	C	10^{-6}	--	--
LH_2	413,700 (60)	TVS	24	C	10^{-6}	1	1.27 (0.5)**
LH_2	413,700 (60)	TVS	24	C	10^{-6}	1	1.27 (0.5)†
LH_2	413,700 (60)	CP	24	C	10^{-4}	--	--
LH_2	413,700 (60)	CP	6	C	10^{-6}	--	--
LH_2	413,700 (60)	CP	12	C	10^{-6}	--	--
LH_2	68,950 (10)	TVS	24	C	10^{-6}	1	0.64 (0.25)[a]
LH_2	68,950 (10)	TVS	24	C	10^{-6}	1	0.64 (0.25)[b]
LH_2	206,900 (30)	TVS	24	C	10^{-6}	1	0.64 (0.25)[c]

*CP = constant pressure
COMP = compression
TVS = thermodynamic vent system condensation
PL = pleated liner; C = channel

**$\dot{W}_v$ = 10%
†$\dot{W}_v$ = 20%
[a]Fluid properties at 103,400 N/m^2 (15 psia)
[b]Fluid properties at 208,900 N/m^2 (30 psia)
[c]Fluid properties at 344,800 N/m^2 (50 psia)

Table 6

TYPICAL FILL PARAMETERS

Mass Summary

		kg	lb
Total Mass In	=	38.92	85.80
Chilldown Mass	=	0.388	0.855
Liquid Mass in System	=	38.53	84.94
Liquid Mass in Screen	=	0.336	0.742
Liquid Mass in Tank	=	38.17	84.14
Vapor Mass in Tank	=	0.025	0.054
Pressg Gas Mass in Tank	=	0.	0.
Mass Vented	=	2.37	5.22

Event Summary

Chilldown s' s	-48,244 sec
Chilldown complete/fill starts	0 sec
Screen device wicked over	751 sec
Ullage bubble established	825 sec
Tank filled	86,901 sec

Stability/Weber Numbers

Inflow	16.5
Screen device	0.175×10^{-3}
Tank	0.224×10^{-8}

NOTE: 24-hr fill of 0.62-m^3 (22 ft^3) Spacelab LH_2 tank with channel screen device at 413,700 N/m^2 (60 psia) and 10^{-6} g's.

Table 7

VOLUME OF GAS TRAPPED IN SCREEN ACQUISITION DEVICE DUE TO WICKOVER

Fluid	Trapped Gas Volume (m^3)	% of Screen Volume
LH_2	5.49×10^{-6}	0.102
LO_2	4.11×10^{-6}	0.076
MMH	2.29×10^{-6}	0.043
N_2O_4	3.65×10^{-6}	0.068

NOTES:
1. Multiarm screen channel
2. Total screen device volume = 5.38×10^{-3} m^3
3. Gravitational environment 10^{-6} g's
4. 24-hour fill

Three tank fill methods were considered in this analysis, namely:

1. Constant ullage pressure and temperature – ullage vapor (only) is assumed to be vented overboard during fill.
2. Locked-up (unvented) tank with no heat and mass transfer between the liquid, ullage, and tank during fill.
3. A thermodynamic vent system that condenses only ullage vapors during fill.

The constant pressure or continuous vent method of fill requires that a stable liquid-vapor interface be maintained and its location be known to prevent liquid venting. This analysis considered the liquid-vapor interface stability for flow into the system, the screen device, and through the screen into the tank. Table 8 tabulates the Weber numbers that delineate liquid-vapor interface stability as functions of fill time. The discussion under SUBROUTINE STBLTY noted that a Weber number of 84 or less for the flow into the system delineates a stable liquid-vapor interface. If this were true, then the initial filling of the tank would have to correspond to a flowrate equivalent to a fill time of 10.6 hours or more. However, it is not clear that stability in the inflow line is necessary for stable tank filling, especially after the baffle volume is filled.

Table 8

WEBER NUMBER FOR LIQUID-VAPOR INTERFACE TABILITY DETERMINATION AS A FUNCTION OF FILL TIME

Fill Time, hr	Flow into the System	Flow in the Screen	Flow into the Tank
6	264	0.0028	$\sim 3 \times 10^{-7}$
12	66	0.0007	$\sim 3 \times 10^{-7}$
24	17	0.00018	$\sim 3 \times 10^{-7}$
48	4	0.000044	$\sim 3 \times 10^{-7}$

Further, for flow in the screen device, Table 8 indicates that very high flowrates, equivalent to a fill time of 19 minutes, would still result in a stable liquid-vapor interface within the screen device. Although this would result in high flow velocities in the inlet line (33 m/sec), it is not clear that stability within the screen device is essential. Instability could only cause premature wetting and wickover of the screen. If venting of the screen device (through the TVS) is accomplished, premature wickover could be tolerated. It appears that low-g testing should be employed to define the required stability criterion.

The fill level is dependent on the type of ullage pressure control selected. For the constant pressure and temperature system (where the ullage vapors are assumed to be vented overboard), the fill level is dependent on the location of the vent line and the liquid-vapor interface shape (or fluid properties and gravitational environment). For the locked up (compression) and thermodynamic vent systems, the fill level is dependent on the starting conditions and the allowable ullage pressure and the effectiveness of the thermodynamic vent system.

Table 9 compares the potential fill levels for the three tank fill methods, assuming a final tank ullage pressure of 413,700 N/m^2 (60 psia). Figures 18 and 19 illustrate the ullage pressure history for the locked-up tank fill and TVS vent methods as a function of the initial ullage pressure. The locked-up fill assuming compression without heat and mass transfer (Figure 18)

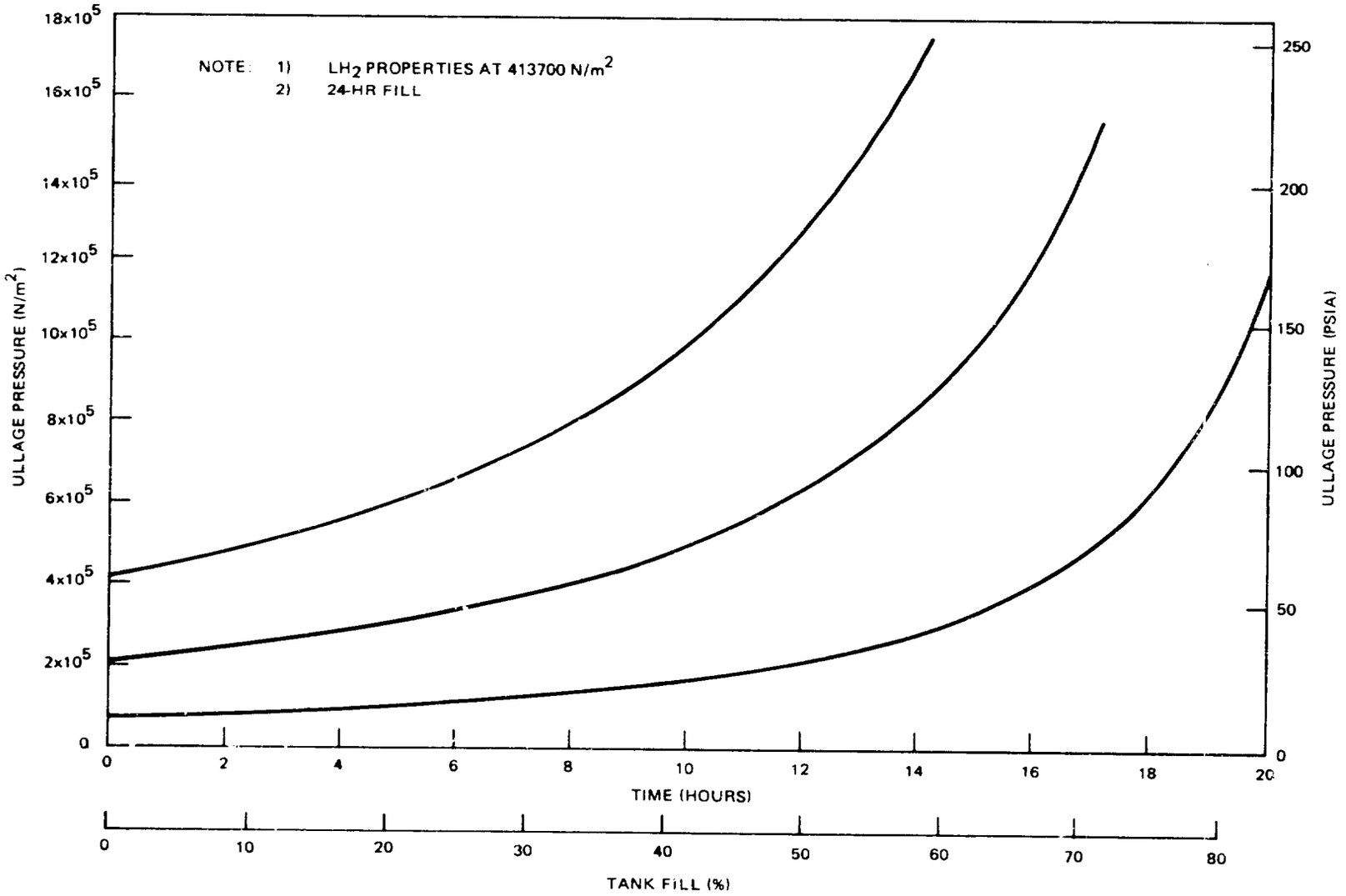

Figure 18. Ullage Pressure History for Compression Without Heat and Mass Transfer as a Function of Initial Ullage Pressure

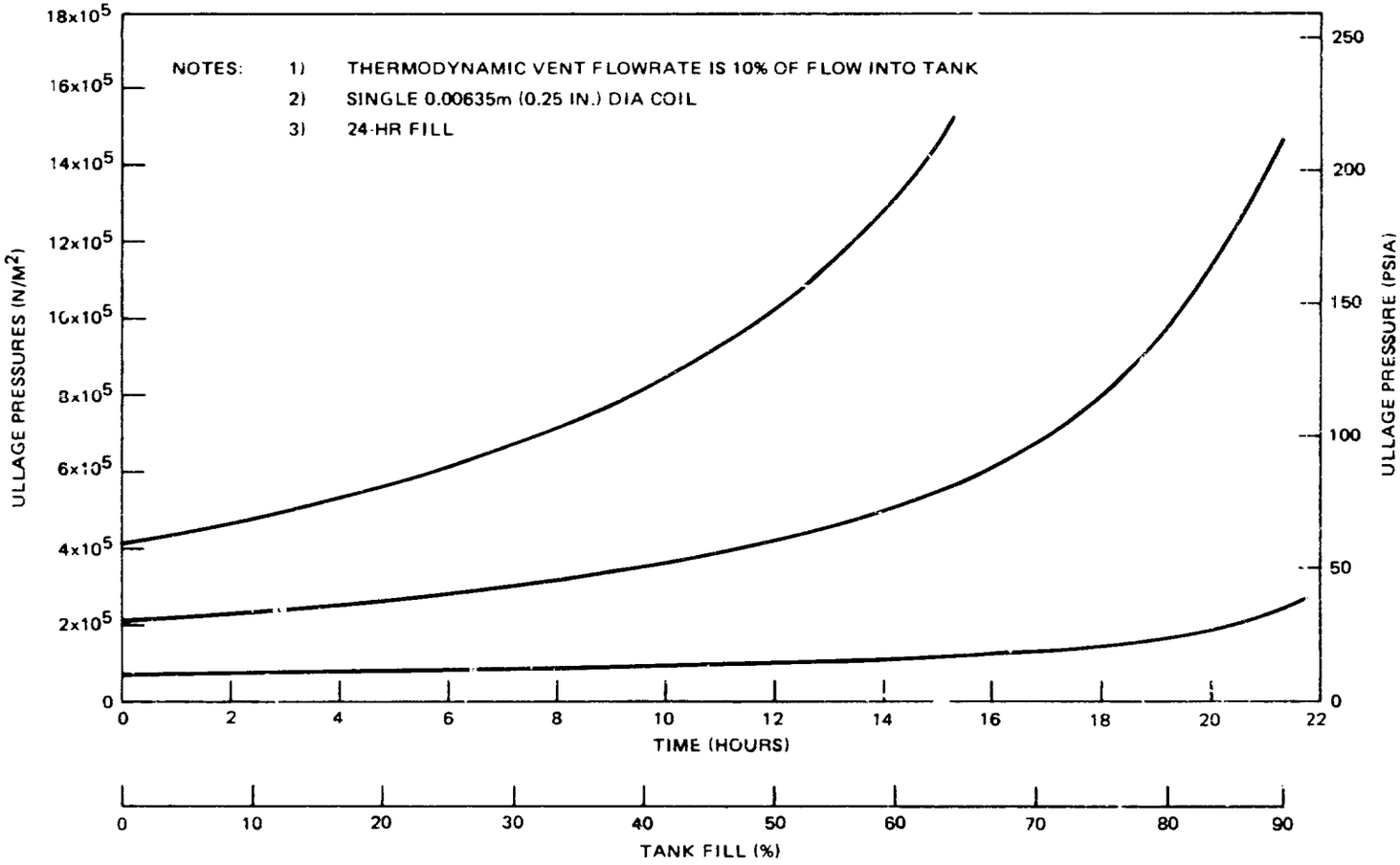

Figure 19. Ullage Pressure History for the Thermodynamic Vent System as a Function of Initial Ullage Pressure

Table 9

COMPARISON OF CONSTANT PRESSURE AND LOCKED-UP TANK FILL LEVELS

	Constant Pressure	Thermo-dynamic Vent System	Compression Without Heat or Mass Transfer
Initial tank pressure (N/m^2)	413,700 (60 psia)	68,950 (10 psia)	68,950
Final tank pressure (N/m^2)	413,700	413,700	413,700
Fill level (%)	99	93	66
LH_2 required (m^3)	0.616	0.639	0.411
LH_2 in tank (m^3)	0.616	0.581	0.411

NOTES:
1. Fill flowrate corresponds to a 24-hour fill time.
2. TVS flowrate is 10% of flow into the tank.
3. Tank is assumed to be prechilled.

appears to be only suitable for low initial ullage pressures and moderate fill evels (about 2/3 full). The TVS vent method (Figure 19) appears to provide fill levels in excess of 90% provided the initial ullage pressure is low. Higher fill levels or higher initial ullage pressures are possible by increasing the fill time and/or increasing the size of the TVS heat exchanger. It appears that the TVS vent method could be a practical technique for orbital filling and warrants further study.

MODELLING AND EXPERIMENT DESIGN

Determining the modelling techniques appropriate for experimental evaluation of the critical processes occurring in orbital fluid management system filling, requires definition of: (1) the important characteristic dimensionless numbers for the process, and (2) the experimental regimes as a function of the gravitational environment. The experimental regimes can be separated into (1) ground-test experiments, (2) drop-tower experiments, and (3) long-term orbital experiments.

Ground Test Experiments - These tests would be used to evaluate processes characterized by dimensionless numbers not involving local gravity. Examples are forced convection heat transfer, as for chilldown, or thermodynamic vent operation.

Drop-Tower (or Aircraft) Experiments - These tests would be used to characterize processes in which low-gravity was required because the characteristic dimensionless numbers included surface tension (such as We or Bo), but in which dimensional scaling and simulant-fluids could provide appropriate phenomena development and scaling within the short low-g durations (5 to 30 sec) available. Examples are inflow interface stability into and through screen devices.

Long-Term Orbital Experiments - These tests would be used to characterize those processes requiring long periods of low-gravity. Examples are low flowrate filling interface stability and thermodynamic fill vent ullage condensation processes.

Each process involved in filling was examined in turn, to evaluate the appropriate characteristic dimensionless numbers.

CHILLDOWN

The configuration of the Spacelab fluid management system is such that essentially all of the metallic mass to be chilled down inside the tank is concentrated

in the tank wall and the screen device. All of the initial fluid inflow is essentially confined to the screen annulus or channel. With the liner, all of the vaporized fluid (gas) will tend to flow along the annulus in contact with wall and liner, and through the liner, tending to use all its heat capacity for chilldown. Similarly, for the channel configuration, the vaporized inflow will flow through the screen and along the tank wall also tending to use all of its heat capacity. Because of the low inflow rates, it is believed that the chilldown process will approximate, more closely, the case where the minimum chilldown fluid requirements occur because the chilldown fluid exits the system at the equipment temperature (previously shown as σ_{min} in Figure 3). The actual chilldown mass is defined as a factor, f, times the σ_{min} from Figure 3 and Reference 8

$$M = f \cdot \sigma_{min} \cdot M_{equip} \tag{86}$$

based on the metal mass chilled down, M_{equip}, and the initial temperature. If chilldown inefficiencies occur, f would have a value greater than 1.0.

Although Equation (86) is used to determine the fluid mass required for chilldown, the generalized Nusselt expression for heat transfer coefficient for forced convection defines the heat transfer rate between the cool vapor and the warm metal. The expression is

$$\frac{h_c d}{k} = C \left(\frac{\rho V d}{\mu}\right)^b \left(\frac{C_p \mu}{k}\right)^a \tag{87}$$

where

$\frac{h_c d}{k}$ = Nusselt number

$\frac{\rho V d}{\mu}$ = Reynolds number

$\frac{C_p \mu}{k}$ = Prandtl number

The constants a, b, and c depend on the type of flow (laminar or turbulent), type of surface (flat plate, vertical wall, horizontal wall, pipe, etcetera), type of fluid (liquid or gas), and direction of heat transfer (cool fluid, warm fluid, etcetera).

The Prandtl number for gases is usually of the order of 0.7, which is the case for cryogenic fluids such as hydrogen, oxygen, and nitrogen (although the values are not the same).

For gaseous hydrogen in the inlet pipe (d = 0.0053m) at 413700 N/m^2, 56 K, and assuming the liquid hydrogen flowrate required to fill the tank in 24 hr (~1.6 Kg/hr), the Reynolds number is 39000., indicating a highly turbulent flow. But the corresponding Reynolds number in the screen device of the full pleated liner is about 75., indicating laminar flow. This range of Reynolds number indicates that the heat transfer coefficient may differ significantly in various parts of the system.

Since the heat exchange in the chilldown process is between the vapor and metal (no liquid in the system), the chilldown process is independent of local acceleration, thus normal-g testing can be done to: (1) verify that the chilldown is complete before liquid fill begins, (2) verify the efficiency of the heat exchange/transfer to determine the value of f in Equation (86), and (3) determine the flow path of the chilldown gas (i.e. does it flow along the screen device and exit at the opposite end) by measuring the temperature history in different parts of the tank.

SCREEN FILLING

The screen filling process is assumed to be a function of the inflow rate stability, the screen wicking model, and the flow and pressure distribution model in the screen device.

The inflow rate stability considers the stability of the liquid-vapor interface as it enters and flows into the tank. This phenomenon is generally characterized by a Weber number based on inlet line radius and average inflow velocity.

The stability of the vapor interface with the liquid that flows in the liner and through the screen was analyzed, based on considerable work accomplished

by NASA-LeRC in developing correlations for liquid-vapor interface stability criteria for flow into various kinds of tanks. None of this work was specifically directed toward flow into or through screens, so that the correlations obtained for other configurations were carefully reviewed and analyzed to determine their applicability to the problem of screen flow.

Stability criteria defined by a Weber number based on inlet line radius and average inflow velocity into an initially empty hemispherical-ended cylinder in zero gravity (References 10 and 11), have shown stable inflow at Weber numbers of about 1.3. Weber number stability criteria determined for a partially full hemispherical-ended cylinder during weightlessness (Reference 12), indicated stability at Weber numbers of about 1.5.

The Weber number stability criteria for a baffled spherical tank (Reference 13), indicated stability for Weber numbers of about 3 to 16 based on the inlet line radius and average inlet line-flow velocity. The comparison of different types of baffle configurations (Reference 14), indicated that inflow velocities could be increased by 2 to 11 times depending on the type of baffle used (see Figure 11). Because Weber number is proportional to velocity squared, the increase in Weber number for a stable flow is 4 to 121 times greater than that for the unbaffled tank, shown to be 1.5. Thus, there is reasonable consistency between References 13 and 14.

The Weber number for the Spacelab tank for a 24-hr fill based on the inlet line-flow velocity and radius is about 16. Therefore, even assuming a plain disk baffle configuration for our system the liquid-vapor interface would probably be stable, although the analysis currently assumes a more complex stacked disk configuration with a stable flow Weber number of 84.

Because no previous work has been done with flow into a screen device, low-g testing should be conducted to delineate the Weber number stability criteria for the full pleated liner and screen channel configurations.

Drop tower experiments with scaled tanks and screen devices would provide the most cost-effective method for determining the inflow rate stability criteria because of the short duration of this phenomena, the requirement for visual observations of the experiments with photographic equipment, and the potential

for conducting a number of tests. Simulant fluids with dynamically similar surface tension and density properties would be required to simulate the cryogenic and storable fluids.

The screen wicking model, developed in Reference 17, is expressed as

$$V_w = \frac{C_s}{L} \frac{\sigma}{\mu} - C_s \frac{\rho a}{\mu} \frac{D_p}{\phi} \sin \alpha \qquad (88)$$

This model is used to determine the wicking front distance relative to the fluid front and thus, the time at which wickover occurs. The Reference 17 liquids employed in the experimental investigation were methanol and ethanol. The fluid properties for these two liquids and the liquids (LH_2, LO_2, MMH, N_2O_4) to be considered in this analysis are tabulated in Table 10. Also shown are the ratios σ/μ and ρ/μ. As is readily apparent, the Reference 17 test fluids compare fairly well with the fluids to be considered in this analysis, therefore low-g experiments could be conducted to verify the applicability of the screen correlation constants developed in Reference 17. Low-g experiments can be simulated by positioning the test specimen at a near horizontal position so that the value of a sin α is of the 10^{-4} to 10^{-6} g order of magnitude. This would require near zero angles (α = 0.0001 - 0.000001 rad)which may be difficult to achieve, therefore, drop tower or aircraft testing may be required.

The screen device flow model is a function of the capillary pressure at the liquid-vapor interface, the frictional losses along the screen device, and the screen device geometry.

The capillary pressure [$\sigma \left(\frac{1}{R_1} + \frac{1}{R_2}\right)$] is a function of the fluid surface tension and flow cross-sectional area configuration and cannot be readily characterized by a dimensionless number. The magnitude of the capillary pressure with respect to frictional losses, dynamic pressure changes, and head pressure in low-g, provides the basis for the determination that the screen device will be completely filled before flow through the screen and into the main tank begins. Because these values are several orders of magnitude smaller than the supply and ullage pressures (see Table 11), low-g experiments of long duration would be required. Low-g is required to provide low head pressures and long duration (low flowrates) is required to provide small frictional losses.

Table 10

FLUID PROPERTIES

Fluid	Temperature (K)	Property: Density (Kg/m^3)	Property: Surface Tension (N/m)	Property: Viscosity ($N\text{-}sec/m^2$)	Property: σ/μ (m/sec)	Property: ρ/μ (sec/m^2)
Ethanol	293	789.8	0.0223	1.20×10^{-3}	18.6	6.59×10^{5}
Methanol	293	793.0	0.0226	5.97×10^{-4}	37.9	1.32×10^{6}
LH_2 at (saturated)	26	62.6	0.0010	1.06×10^{-5}	94.3	5.90×10^{6}
LO_2 at (saturated)	106	1057.3	0.0093	1.30×10^{-4}	71.5	8.14×10^{6}
MMH	293	876.3	0.0343	8.56×10^{-4}	40.1	1.02×10^{6}
N_2O_4	293	1447.2	0.0266	4.17×10^{-4}	63.8	3.48×10^{6}

Table 11

PRESSURE VALUES DURING SCREEN FILLING

	Pleated Liner N/m^2
Ullage Pressure	413700.
Supply Pressure	~413700.
Capillary Pressure at θ = 2.9 rad	3.05
Frictional Loss ($\Delta\theta$ = 2.65 rad)	0.2
Head Pressure at Inlet	0.00063
Dynamic Pressure at Inlet	0.00009

The frictional losses through the screen device can be characterized by the Reynolds number. The frictional loss models are based on the Reference 2 and Reference 1 analysis and experiments for the full pleated liner and screen channel configuration, respectively.

TANK FILLING

The tank filling process is assumed to be a function of the liquid-vapor interface stability, the screen flow-through model, and the liquid distribution model.

In order to successfully fill the tank, especially when venting is required, or the thermodynamic vent system is used, the liquid-vapor interface in the tank has to be stable so the liquid shape and location can be predicted with some accuracy. Generally the liquid-vapor interface stability criteria are characterized by the Weber number. The subsequent aspects of the tank filling process assumes a stable liquid-vapor interface.

Determination of the proper characteristic dimension and appropriate velocity to define the Weber number is complicated by the complexity of the flow field through the screen and into the tank. For the pleated liner, the liquid will be weeping through the screen, thus the stability criteria should probably be based on the Weber number with the radius from tank center to screen being

the critical dimension. The flow velocity will be different through each screen segment, thus, for conservatism, the stability criteria should be applied to the largest value of flow velocity.

For the screen channel configuration, the flow into the main tank is even more complex. Referring back to Figure 12, the liquid will first flow into the channel (1), through the screen into the space between the channel and tank wall (2), then through the side of the channel into the main tank (3). The flow into the main tank will then merge with the flow from the adjacent screen channel and flow toward the center of the tank (4). The Weber number stability criteria are thus assumed to be based on the distance between screen channels and the maximum inward velocity between the channels.

The liquid-vapor interface stability of the fluid mass inside the main tank is critical, if the tank is being vented during the fill process in order to maintain a reasonable system pressure. An unstable interface could result in liquid venting. The complex nature of the flow makes it difficult to ascertain the flow velocity distribution or Weber number stability criteria. Low-g testing should be done to obtain the actual Weber number that delineates liquid-vapor interface stability.

The screen flow-through model is developed in Reference 1 and is expressed as follows for screen flow-through velocity, V,

$$V = \frac{\sqrt{A^2 + 4\,B\,\Delta P} - A}{2B} \tag{89}$$

where ΔP = pressure drop across the screen

A and B are constants determined in Reference 1.

This model can be characterized by the dimensionless Reynolds number. The Reynolds number for the flow through the pleated liner assuming the 24-hr Spacelab tank fill rate is about 0.01. Thus, the flow is highly laminar or in the region where the friction factor is a linear function of A and the Reynolds number. Therefore, the results from Reference 1 can be used with confidence.

The screen wicking model is developed in Reference 17, and is expressed as Equation (88), previously shown.

This model is used to determine the shape of the liquid flowing into the tank. The analysis assumes that the liquid-vapor interface will have a spherical shape because of the low energy associated with the flowing liquid. The apparent wicking along the screen will drag the fluid front along so that, at any given time, the chord of the liquid-vapor interface can be approximated by the wicking front. This process continues until the wicking front completely encircles the tank, enclosing the ullage.

The spherical shape or the near-spherical shape of the liquid in the tank, can be characterized by the dimensionless Bond number $\left(\frac{\rho a R^2}{\sigma}\right)$ where R is the radius of the spherical ullage bubble. An analytical model was developed (Reference 15) indicating near-spherical shapes for Bond numbers of about 5 or less.

Preliminary calculations for the Spacelab tank system indicate Bond numbers between 0.13 and 0.70 for a local acceleration of 10^{-6} g's. Therefore, the surface tension forces are dominant and the assumption of a spherical ullage bubble appears justified.

Long durations (~800 sec) are required for the ullage bubble to be completely enclosed by liquid clearly indicating that this process cannot be adequately simulated with realistic scaling in the short duration low-g environment available from drop towers or aircraft.

The complex nature of the flow-field through the screen and into the tank, as discussed previously, makes it difficult to identify the proper characteristic dimension and appropriate velocity for the determination of the Weber number. Therefore, it is believed that the appropriate way to model the process is through the use of full scale hardware (perhaps with simulant fluids used to model σ/ρ) in a low-g experiment. Because liquid-vapor interface stability is generally determined visually, a plexiglass tank (or tank window) with photographic coverage would be desirable. Orbital low-g experiments appear to be necessary because of the long duration required to fill the screen device upstream volume, before liquid starts to flow through it. For example, if the

screen device of the test model was limited to the one-degree section that preliminary calculations have indicated would be required to pass the liquid through the screen, it would take about 65 sec to fill the screen device upstream volume (screen volume + baffle volume) assuming the flowrate for the 24-hr Spacelab tank fill time. However, it may be possible to fill the screen first, and then drop the experiment in a drop tower.

The ullage conditions and venting associated with filling are thermodynamic effects basically depending on heat transfer processes. The ullage gas temperature and pressure depend strongly on the incoming fluid condition, the degree of stratification and/or ullage mixing, and the presence of cold or hot spots within the tank. Because the inflow process is envisioned as quite slow and the liquid interface as stable, there could be minimal gas mixing leading to substantial stratification effects. Because of the fill vent TVS tube, the stratification could be further affected by the cold region in the liquid. As a result, the assumption of mixed ullage may not be accurate and the actual vent requirements and/or ullage pressure history may be significantly different.

Stratification is strongly dependent on: (1) the local g-field, (2) the characteristic time, θ, (3) the characteristic dimension, D, (4) the heat flux, q, and (5) the fluid properties (Reference 18). The important dimensionless numbers used for process modeling are the Fourier number, $\mu\theta/\rho D^2$, the modified Grashof number, $g\beta qD^4\rho^2/k\mu^2$, the interface parameter, $qDc_p/h_{fg}k$, and Prandtl number, $c_p\mu/k$. For tests using the same fluid with the same properties, the scaling requirements are that θ/D^2, gD^4q, and qD must be scaled for similarity. These groups imply that for a one-g test to simulate 10^{-6} g's, the test system D must be 100 times the low-g system D, the test q must be 10^{-2} times the low-g q, and the test characteristic time θ must be 10^4 times the low-g θ. It is unlikely that these scaling requirements can be met, hence, a long-term low-g test, as in Spacelab, would be required.

The operation of the fill-vent TVS depends on heat transfer processes which are probably g-dependent. The two-phase flow and heat transfer occurring in the TVS heat exchanger depends on the flow regime (mist, annular, froth, slug, et cetera) which in turn may be influenced by the g-field. Most correlations show no g-dependence, but clearly some flow regimes, such as slug

flow may be g-dependent, and perhaps would not even occur in low-g. Further, regime transition flowrate may also be affected by g-level. Normally, the times required to allow flow process stabilization, especially at very low flowrates, is longer than available from drop tower or aircraft tests (Reference 19), therefore long-term low-g experiments (e.g. using Spacelab) should be performed to determine flow regimes and heat transfer and pressure drop correlations as a function of mass velocity (as recommended in Reference 19).

The condensation process occurring on the outside of the TVS heat exchanger is clearly sensitive to gravity as it affects condensate film removal, described in Reference 20. Whether or not surface tension forces can effectively remove the liquid film in low-g can only be resolved by a long-term, low-g experiment (e.g. in Spacelab). The effect of a two-component ullage (including a noncondensable gas) on the condensation performance in low-g is also unknown. It is possible that the noncondensable gas may blanket the condenser in the absence of mixing or buoyancy (g-force) effects and prevent condensation of ullage vapor, except that penetrating the noncondensable gas by diffusion. It is possible that an indication of this blocking effect could be determined with one-g tests, even though buoyancy effects between, for example, helium and H_2 vapor would be significant. The actual performance degradation due to gas blocking would, of necessity, be determined with long-term, low-g experiments (again, in Spacelab, for example).

Based on the modeling techniques resulting from the consideration of process characteristics described above, a detailed evaluation was performed of the experimental program needed to define critical aspects of the filling process for orbital fluid management systems. The experiments required are categorized as: (1) ground tests, (2) drop tower (or aircraft), and (3) long-term orbital.

GROUND TESTS

There are two areas amenable to one-g experiments or ground tests, tank/screen chilldown and fill vent TVS exploratory tests.

Tank/Screen Chilldown: The chilldown process, because it is strongly dependent on chilldown mass and configuration, is best studied using the actual tank/screen configuration with LH_2, and with representative thermal control/heat flux rates. This test would best be performed as part of the tank development and qualification process, and would characterize the expected chilldown parameters for both ground and orbital chilldown. The objectives of this test are:

1. Determine the degree of efficiency of tank/screen chilldown before liquid enters the screen device.
2. Determine the temperature histories of vent gas and tank/screen system.
3. Determine the required chilldown fluid mass.
4. Determine the tank pressure history for constant chilldown flowrate.
5. Determine the performance of the chilldown vent.
6. Determine the thermal control system (MLI-VCS) chilldown performance.

Details of required instrumentation, procedures, and appropriate costs are described for the SCFME in Reference 7.

Exploratory Fill Vent TVS Tests: The performance of the fill vent TVS heat exchanger is highly g-dependent, as discussed above. There are several aspects of the performance characterization that can be experimentally evaluated in one-g in an exploratory way, and which would shed much light on the characteristics and practicality of this vent technique.

The objectives of these exploratory tests are:

1. Determine the TVS heat exchanger heat transfer performance as a function of exposed length and vent downstream pressure.
2. Determine tank pressure history and correlation with inflow rate and TVS performance.
3. Determine performance degradation due to noncondensable gas blockage as a function of initial gas concentration.

During the tests, it would be convenient to study locked-up (unvented) tank filling (after chilldown).

The basic apparatus should consist of a plastic channel with screen windows and a TVS fill-vent of plastic installed in an approximate 0.61-m dia transparent tank (Figure 20), and tested with Freon-114 as a condensable simulant fluid. The screen channel should be fabricated from 0.003-m thick plexiglass sheet and configured as shown in Figure 21. A series of nine 0.076-m square windows in the channel should face the tank wall and should be covered with pleated (in the flow direction) 325 x 2300 mesh stainless steel screen bonded to the plexiglass window frames with polyurethane adhesive. The ends of the pleated windows should be coined flat and bonded to the inside of the channel window to reduce the tendency for bubble trapping at the window edges. The plexiglass back of the channel would allow viewing into the channel from outside the tank. The top of the channel should include an outflow line and a TVS viscojet for simulating TVS venting during inflow and chill-down. Also included in the tank should be a plastic TVS vent line with an integral viscojet. The viscojets should be sized to provide the correct relative flowrate with Freon-114 as occurs with the SCFME tank LH_2 viscojets. The channel should be curved to fit the test tank wall curvature, and attached to the test tank at the top and bottom of the channel to provide a snug fit.

The test tank shells should be thick enough (ranging from about 0.013m to 0.0076-m) to allow a 344750 N/m^2 working pressure level in the tank. Use of a girth ring allows for fluid inflow/outflow lines, instrumentation wiring, et cetera, while use of plex 55 shells would allow superb viewability. The plex 55 material is very strong, resistant to Freon-114, and has been used with LH_2 at low pressures. The test tank should be vacuum- and pressure-proof-tested to assure safe usability during the test program.

The arrangement of the test tank, screen device, plumbing, and instrumentation is shown schematically in Figure 22. Inflow is from the Freon-114 tank, pressurized with helium, as necessary to effect transfer. Negative one-g outflow from the channel should pass through a plastic bubble trap to catch vapor (if any), and returned to the vented Freon-114 tank. Helium pressurization should be used for test tank outflow, and the same line used to evacuate the tank for unvented fill. A vacuum pump should also be used to provide low pressure for fluid expansion through the TVS viscojets and the thermodynamic fill venting viscojet. The instrumentation which should be used in the test

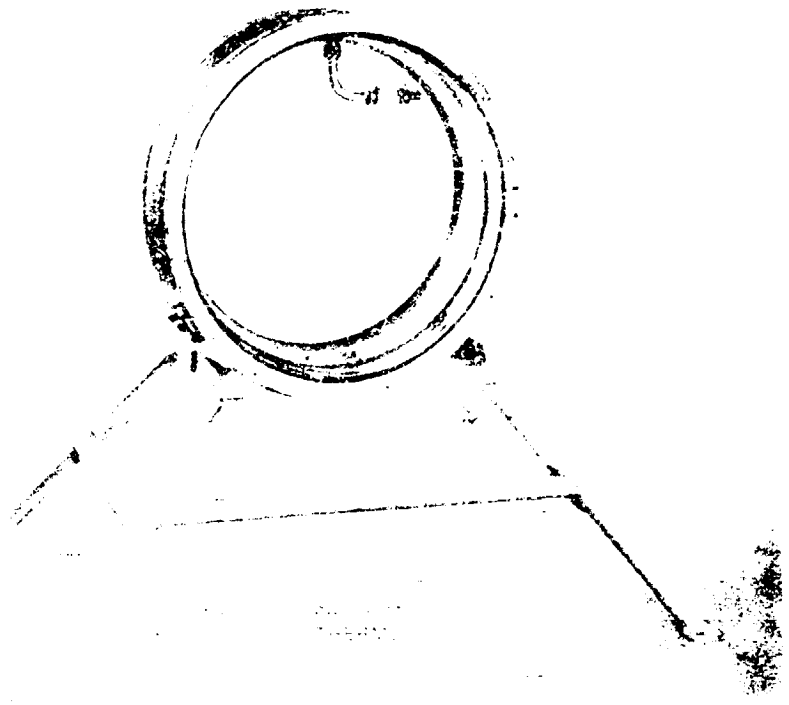

Figure 20. 0.61-m Diameter Test Tank

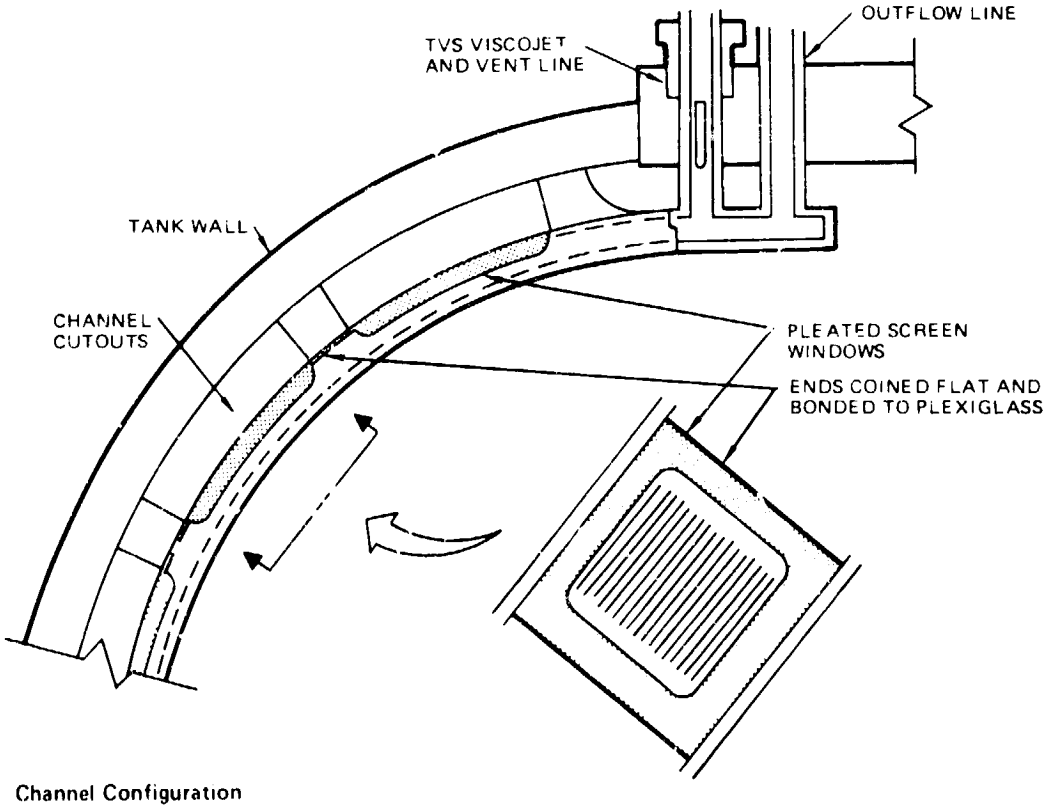

Figure 21. Channel Configuration

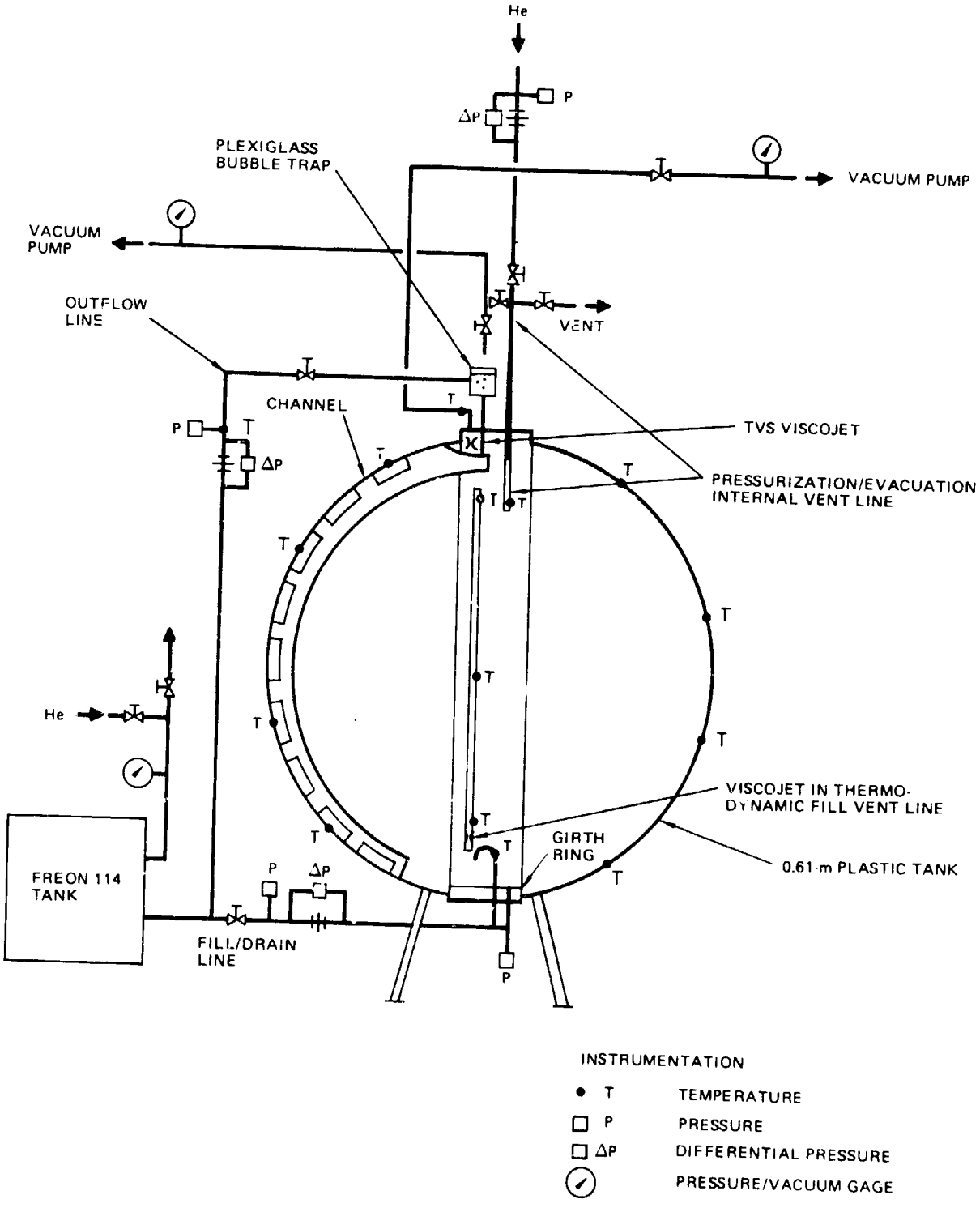

Figure 22. Test Aoparatus Schematic

apparatus is listed in Table 12, and consists of standard copper/constantan thermocouples, pressure transducers, differential pressure transducers (for flow measurement), and pressure/vacuum gages. The data from all of these transducers would be recorded on an oscillograph. Photographs should be taken of interesting phenomena occurring during the test program.

The test matrix should consist of several fill/drain cycles integrated to obtain the maximum information and data with minimum testing. Two basic fill flowrates are anticipated: a typical Spacelab tank ground fill (volumetric) rate for one-hr fill (which would fill a 0.61-m tank within 10 min), and the possible orbital Spacelab tank fill rate for 10 to 24-hr fills (which would fill the 0.61-m tank in 1.7 to 4 hr).

The Freon-114 fluid temperature should be adjusted to at least two values so that a range of post-chilldown heat flux can be simulated: saturated at 10^5 N/m^2 (277K) and, for example, saturated at 1.38×10^5 N/m^2 (285K), depending on ambient temperature. Filling the experiment tank should be done with the tank warm (~292K) and chilled down (~277K). The pressure during filling, while venting, will depend on the Freon-114 fluid

Table 12
INSTRUMENTATION REQUIREMENTS

Parameter	No.	Transducer
Tank Temperature	8	Cu-Cn Thermocouples
Fluid Temperature	2	Cu-Cn Thermocouples
Pressurant (He) Temperature	1	Cu-Cn Thermocouples
TVS Viscojet Temperature	2	Cu-Cn Thermocouples
Fill-Vent Heat Exchanger Temperature	3	Cu-Cn Thermocouples
Pressurant (He) Flowrate	1	Pressure, Differential Pressure
Outflow Rate	1	Pressure, Differential Pressure
Inflow Rate	1	Pressure, Differential Pressure
Tank Pressure/Vacuum	1	Pressure, Vacuum Gage
TVS Viscojet Vacuum	2	Vacuum Gage
Fill-Vent Heat Exchanger Vacuum	1	Vacuum Gage

saturation temperature; it is anticipated to be in the range of 1 - 1.38 x 10^5 N/m^2. During evacuated unvented fill, the pressure excursions could exceed this range, and should be monitored as a test parameter. There are three initial fill levels within the tank which would occur naturally during the test program: (1) empty, (2) at the bubble point level (as a result of previous outflow to the point of screen breakdown), and (3) at the wickover point (~90 to 95% full) when topoff would occur.

With these basic test parameters and the tank configuration inverted as shown in Figure 23, the following test operations are envisioned:

1. With the tank initially warm, the tank and channel section are filled at the ground inflow rate through the ground fill/drain line (while venting through the internal tank vent and the channel TVS vent) until the initial fill level is reached.
2. After simulated thermal control system chilldown (post-fill external heat flux) and topoff as required, initiate outflow (at ground fill rate) against negative one-g until channel breakdown occurs.
3. Drain through the ground fill/drain line until tank is nearly empty. Vacuum pump tank to internal pressure of about 7000 N/m^2 absolute, with internal tank vent closed.
4. Fill the tank at orbital inflow rate (unvented, except for TVS venting from channel).
5. After simulated thermal control system chilldown (post-fill heat flux) and topoff as required, initiate outflow through channel (at orbital outflow rate) against negative one-g until channel breakdown occurs.
6. Allow Freon-114 to saturate at 1.38 x 10^5 N/m^2 and fill the tank and channel at the orbital inflow rate while venting internally through the thermodynamic fill vent and TVS venting from channel.
7. After simulated thermal control system chilldown (post-fill heat flux) and topoff as required, initiate outflow through channel (or orbital outflow rate) against negative one-g until channel breakdown occurs.

The above sequence could be repeated with different fluid saturation pressures and temperatures which would complete the required matrix conditions. In the basic sequence above, the screen device is filled and emptied three times

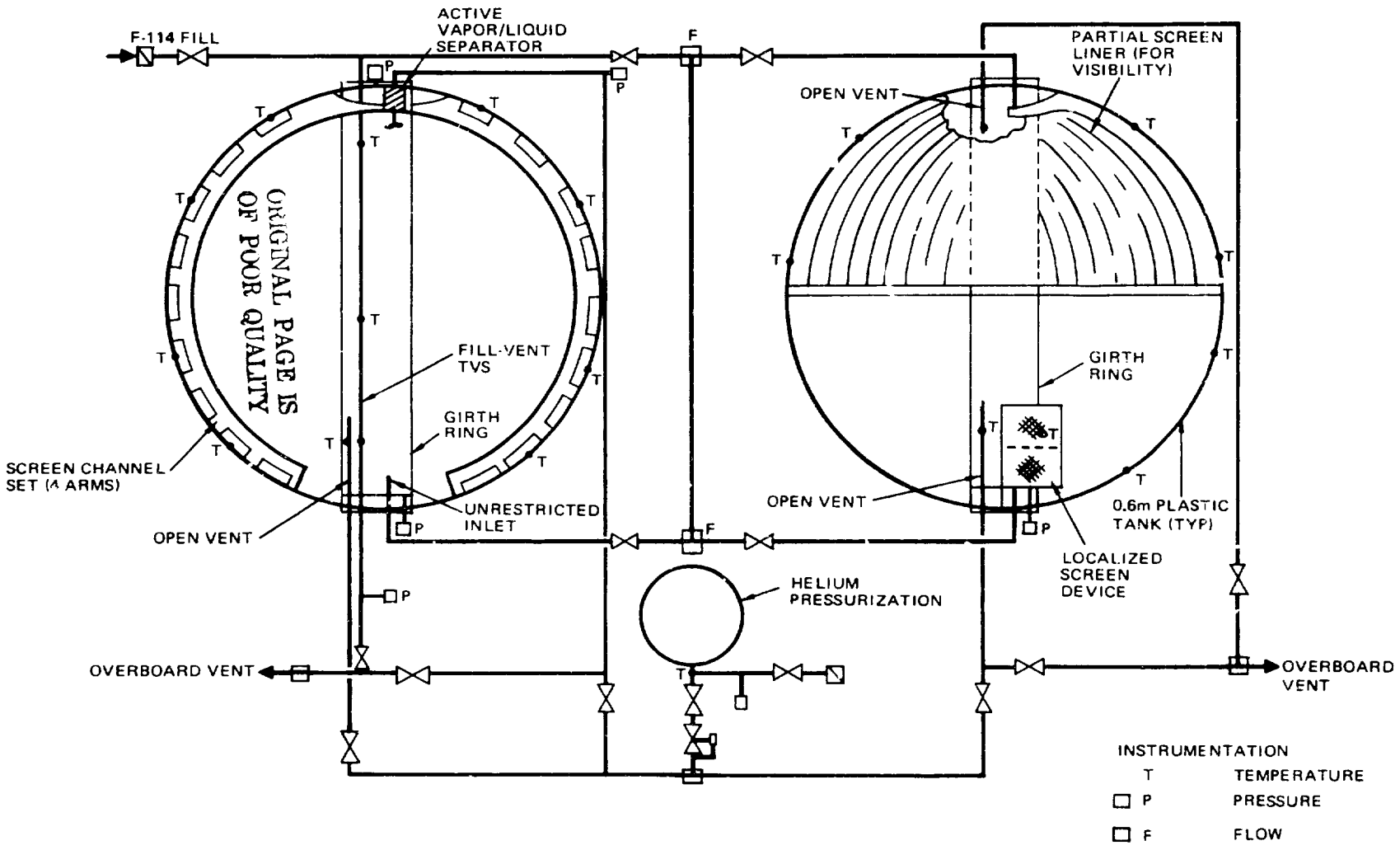

Figure 23. Spacelab Venting/Refill Experiment Schematic

at varying conditions. The important aspects of each phase of this test program/matrix would be determined by observing the process in the test tank and monitoring relevant instrumentation. During filling through the ground fill line in the inverted configuration, item (1) above , the tank chilldown rate should be monitored as a function of time by observing the tank thermocouples. As the screen device fills, it would be observed to determine bubble migration and the wickover point. During the external heat flux (simulated thermal control system chilldown), bubble generation within the channel would be monitored. The ability of the TVS vents and the internal tank vent to remove generated bubbles would be verified during this phase and topping off while venting through the outflow line.

When it appears that negative one-g outflow can be reliably initiated, that phase of the experimental process would be visually monitored. The purpose of this aspect of the test program is to assure successful screen device/tank filling, as proven by the capability of performing negative one-g outflow. If trapped gas affects the retention capability of the screen device, its effect should be noted in the test and the helium pressurant requirements for outflow recorded and compared with the predicted requirements.

The orbital filling processes, both following evacuation (unvented) and using thermodynamic venting during fill, would be conducted to determine fluid behavior and tank pressure history. The filling (or failure to fill) the screen channel and tank would be monitored, and the propensity of the screen device to trap gas, plus the ability of the TVS vents to remove this gas, would be observed. The performance of the unvented fill method would be closely watched; inflow-rate modifications may be required to maintain tank pressure at acceptable levels. The final fill level in the tank, and in the screen device, would be noted as a function of tank pressure and inflow rate. TVS venting rate is also a function of tank pressure, and would be monitored.

Temperature, pressure, and flow-data in the thermodynamic vent heat exchanger would be monitored and recorded. The tank pressure would be monitored and the inflow adjustments required to maintain reasonable tank pressures recorded. The variation in apparent heat transfer coefficient and fill level would be determined for comparison with analytical predictions.

The data which should be recorded or observed, the input/output analytical predictions, and the methods of obtaining correlation between analysis and data are indicated in Table 13. It is estimated that this test program would cost approximately $50,000 (1978 $).

DROP TOWER (OR AIRCRAFT) TESTS

There are also two technology areas which can be experimentally studied using drop towers (or aircraft): (1) stability evaluation for flow through and

Table 13

DATA, ANALYSIS INPUT/OUTPUT, AND CORRELATION METHODS

Data

1.	Inflow rate and conditions	Measurements
2.	Outflow rate and conditions	
3.	System pressures	
4.	System temperatures	
5.	Wicking velocity vs fluid advance velocity	Visual and Photographic Observation
6.	Wicking velocity after fill stop	
7.	Distance between fluid advance front and wicking front	
8.	Wickover/trapped gas	
9.	Bubble generation (quantity)	
	A. Size	
	B. Shape	
10.	Fill level	

Inputs to Analysis

1. Inflow rate and conditions
2. Outflow rate and conditions (experimental or assumed data)
3. Assume heat inflow or calculate from bubble generation and vent flowrate

Output from Analysis

1. System pressure
2. System temperature
3. Wicking velocity vs fluid advance velocity
4. Distance between fluid advance front and wicking front
5. Wickover/trapped gas quantity
6. Bubble generation – quantity
7. Fill level

Correlation Methods

1. System pressure/temperature: adjust heat input, vent flowrate, chilldown mass factor
2. Wicking velocity: adjust screen correlation constant.
3. Wickover/trapped gas: adjust screen correlation constant, determine methods to reduce problem.
4. Bubble generation: adjust heat flux.
5. Fill level: adjust outflow rate.
6. Venting heat exchanger performance: adjust effective heat transfer coefficient.

along screened devices, and (2) removal of condensate films using surface tension forces.

Screen Flow Stability: Studies of Weber number stability criteria applicable to flow through screens (into tanks) and along screened annuli, channels, et cetera, can best be performed using transparent scaled tanks and simulant fluids with the LeRC 5-sec drop tower, as was done with many previous inflow test programs involving fluid stability. The availability of reliable stability information for screen flow will not only affect small scale cryogenic system refill, but also large orbital propulsion vehicle tankage refill which could include a partial acquisition device. These tests should include screen channels, partial liner (to allow visibility), and partially localized screen devices or baffles. The objectives of these tests are:

1. Determine critical Weber number for stability as a function of screen mesh, flow-through velocity, and geometry.
2. Determine these criteria for flow within a screen device, and through a screen device into a tank.

Based on their extensive previous experience, drop tower apparatus configuration, instrumentation, operations, and approximate costs can best be defined by LeRC.

Condensate Film Behavior: Determination of the characteristics of condensate film removal, using surface tension forces in low-g, probably cannot be accomplished in the short times available in drop towers (~5 sec), but may be possible in KC-135 aircraft low-g tests, providing that the g-forces can be kept small enough (10^{-3} to 10^{-4} g's) to allow surface tension forces to dominate. The tank should be scaled to allow rapid establishment of the low-g ullage bubble shape, and should be transparent using a simulant heat transfer fluid such as Freon-114, so that condensate film behavior can be observed. The objectives of these tests are:

1. Determine condensate film behavior as a function of g-level, and ullage size.
2. Determine overall heat transfer rate as a function of g-level, ullage size and TVS internal pressure.

Because of the relatively short low-g times available, these tests are not as desirable as Spacelab experiments and should only be considered if warranted by the results of the exploratory tests, and shown practical by careful analysis of the characteristic times required for the establishment of the low-g regimes to be studied.

LONG-TERM ORBITAL TESTS

The long-term orbital tests, using, for example, Spacelab, would be performed to study all aspects of low-g filling requiring long periods of low-g time, such as inflow stability within the screen device and tank, low-g wicking, and fill-venting. It is possible that proper operation of the low-g fill process could be demonstrated with an integrated system, such as simply refilling a suitably designed Spacelab Cryogenic Fluid Management Experiment tank in a two-tank test.

Preliminary calculations using the Orbital Filling analysis indicate that chilldown and screen or tank filling stability are not a problem, and initial ground or drop tower testing may confirm this, but the low-g venting process is not well-defined. If the one-g exploratory tests are encouraging it may be desirable to fly a Spacelab experiment to study low-g venting using a transparent tank and a simulant heat transfer fluid, such as Freon-114. The objectives of this test program would be:

1. Evaluate several different kinds of vent, including a fill-vent TVS, active vapor/liquid separator, and simple open vent.
2. Determine performance of various vent techniques, such as continuous venting, intermittent fill/venting, and blowdown with locked-up fill.
3. Determine fill patterns and stability, both with flow through a screen channel set, a partial screen device (if required for visibility), a localized screen device, and for unrestricted flow into a tank.

The detailed experimental arrangement would depend strongly on the results of the one-g exploratory tests described previously. The arrangement of the experiment tank could be similar to that shown in Figure 23. Two tanks would be required: one would include a screen channel set of 4 arms and an unrestricted inlet, and the other would include a partial screen liner (for visibility) and a localized screen device at opposite ends of each tank. The

instrumentation would depend on the results of the one-g exploratory tests but would be similar to that shown. Clearly, by appropriate operating procedures, every rational combination of screen device and vent system could be tested while flowing Freon-114 back and forth between the two tanks (one launched full and the other launched empty – or with only the screen device full). The tanks could be observed by closed-circuit TV and controlled from within the Spacelab core module. The estimated cost for development and deployment of such a two-tank experiment is approximately $1,200,000 (1978$).

A logical follow-on (or replacement) to the above experiment would be a cryogenic transfer experiment using two SCFME tanks (as described in Reference 7). The estimated cost of such an experiment would be approximately $1,500,000 (1978 $) above the cost of the basic SCFME.

PRECEDING PAGE BLANK NOT FILMED

CONCLUSIONS

A comprehensive program has been performed to analytically study the gravity-dependent refill phenomena for a small-scale tank containing a screen acquisition device and suitable for a SCFME. The analysis is specifically oriented toward screen channel type and full pleated liner type screen acquisition devices, and is suitable for LH_2, LO_2, MMH and N_2O_4 propellants. The analysis considers the filling phenomena of chilldown, screen filling and wickover, tank filling, interface stability, and ullage pressure control and venting. The analysis is completely operational and has indicated the following observations as a result of typical runs of the program with the SCFME configurations:

- The validity of the assumption that the screen device will be filled before flow-through into the tank starts was verified for the long-fill-times and low-g levels assumed.
- Screen wickover is insensitive to the low-g environment because of the moving incoming fluid front (for wicking only along the screen).
- The TVS fill-vent can provide acceptable ullage pressure for 80-90% fill levels depending on initial pressure and filling operational parameters. These results are conservative and are based on the assumptions of no heat and mass transfer. Higher fill levels could be achieved if heat transfer to the cold liquid was accounted for.
- Unvented tank fill can achieve only moderate fill levels depending on initial and final pressure assumptions. Again, higher fill levels could be achieved if heat and mass transfer were assumed.
- For the SCFME, fill times in excess of 12 hr are required to assure interface stability for system inflow using conservative stability criteria.

The processes involved in low-g filling were examined and modelling techniques, appropriate to the experimental evaluation of critical filling phenomena, were defined. The following experimental programs were recommended to explore critical aspects of the low-g tank filling problem:

- Chilldown testing during the ground development tests of the SCFME.
- Exploratory ground tests of the TVS fill-vent and unvented filling methods using plastic tanks and Freon-114 as a simulant fluid.
- Drop-tower tests to determine stability criteria for simulant fluid flow into and through screen devices.
- Spacelab tests of tank fill, refilling, venting and fluid stability using Freon-114 and a pair of plastic tanks with screen channels, a partial screen liner, a localized screen device, and unrestricted inflow line. Venting techniques used would include TVS fill-vent, active vapor/liquid separator, and open vent, operated in the modes of continuous vent, blowdown/unvented fill and intermittent vent/filling.
- Spacelab demonstration of cryogenic fluid transfer using two SFCME tanks, with LH_2, as a follow on to the baseline SCFME supply demonstration.

REFERENCES

1. E. C. Cady. Study of Thermodynamic Vent and Screen Baffle Integration for Orbital Storage and Transfer of Liquid Hydrogen. MDAC Report MDC G4798 (NASA CR-134482), August 1973.

2. E. C. Cady. Design and Evaluation of Thermodynamic Vent/Screen Baffle Cryogenic Storage System. MDAC Report MDC G5979 (NASA CR-134810), June 1975.

3. M. H. Blatt and M. D. Walter. Centaur Propellant Acquisition System Study. GDC Report CASD-NAS-75-023 (NASA CR-134811), June 1975.

4. R. P. Warren. Acquisition System Environmental Effects Study. MMC Report MCR-75-21, May 1975.

5. E. C. Cady. Effect of Transient Liquid Flow on Retention Characteristics of Screen Acquisition Systems. MDAC Report MDC G6742 (NASA CR-135218), April 1977.

6. J. Tegart. Effect of Vibration on Retention Characteristics of Screen Acquisition Systems. MMC Report MCR-77-253 (NASA CR-135264), October 1977.

7. E. C. Cady. Spacelab Cryogenic Fluid Management Experiment. MDAC Report MDC G6552 (NASA CR-135143), November 1976.

8. R. B. Jacobs. Liquid Requirements for the Cool-Down of Cryogenic Equipment. Advances in Cryogenic Engineering, 1962. Vol. 8, p. 529-535.

9. C. M. Spruckler. Liquid Inflow to Initially Empty Cylindrical Tanks in Low Gravity. NASA TMX-2613 August 1972.

10. E. P. Symons. Interface Stability During Liquid Inflow to Initially Empty Hemispherical Ended Cylinders in Weightlessness. NASA TMX-2003, April 1970.

11. E. P. Symons et al. Liquid Inflow to Initially Empty, Hemispherical Ended Cylinders During Weightlessness. NASA TN D-4620, 1968.

12. E. P. Symons and J. V. Staskus. Interface Stability During Liquid Inflow to Partially Full, Hemispherical Ended Cylinders During Weightlessness. NASA TMX-2348, August 1971.

13. C. P. Andracchio and K. C. Abdalla. An Experimental Study of Liquid Flow into a Baffled Spherical Tank During Weightlessness. NASA TMX-1526, April 1968.

14. J. V. Staskus. Liquid Inflow to a Baffled Cylindrical Tank During Weightlessness. NASA TMX-2598, August 1972.

15. L. J. Hastings and R. Rutherford, III. Low Gravity Liquid-Vapor Interface Shapes in Axisymmetric Containers and a Computer Solution. NASA TMX-53790, October 7, 1968.

16. J. B. Blackmon. Design, Fabrication, Assembly, and Test of a Liquid Hydrogen Acquisition Subsystem, NAS8-27571. MDAC Report MDC G5360, May 1974.

17. E. P. Symons. Wicking of Liquids in Screens. NASA TN D-7557, May 1974.

18. Lovrich, T. M. Final Report, Development of Thermal Stratification and Destratification Scaling Concepts. MDAC Report MDC G4753, July 1973.

19. Bradshaw, R. D. and C. D. King. Conceptual Design for Spacelab Two-Phase Flow Experiments. NASA CR-135327, December 1977.

20. Filling of Orbital Fluid Management Systems, Volume 1, Technical Proposal. MDAC Report MDC G6795P, May 1977.